Adaptive Kalman Filters for Nonlinear Finite Element Model Updating

Mingming Song[1], Rodrigo Astroza[2], Hamed Ebrahimian[3], Babak Moaveni[1], Costas Papadimitriou[4]

[1]*Dept. of Civil and Environmental Engineering, Tufts University, Medford, MA, USA*
[2]*Facultad de Ingeniería y Ciencias Aplicadas, Universidad de Los Andes, Santiago, Chile*
[3]*Dept. of Civil and Environmental Engineering, University of Nevada, Reno, NV, USA*
[4]*Dept. of Mechanical Engineering, University of Thessaly, Volos, Greece*

ABSTRACT

This paper presents two adaptive Kalman filters (KFs) for nonlinear model updating where, in addition to nonlinear model parameters, the covariance matrix of measurement noise is estimated recursively in a near online manner. Two adaptive KF approaches are formulated based on the forgetting factor and the moving window covariance-matching techniques using residuals. Although the proposed adaptive methods are integrated with the unscented KF (UKF) for nonlinear model updating in this paper, they can be alternatively combined with other types of nonlinear KFs such as the extended KF (EKF) or the ensemble KF (EnKF). The performance of the proposed methods is investigated through two numerical applications and compared to that of a non-adaptive UKF and an existing dual adaptive filter. The first application considers a nonlinear steel pier where nonlinear material properties are selected as updating parameters. Significant improvements in parameter estimation results are observed when using adaptive filters compared to the non-adaptive approach. Furthermore, the covariance matrix of simulated measurement noise is estimated from the adaptive approaches with acceptable accuracy. Effects of different types of modeling errors are studied in the second numerical application of a nonlinear 3-story 3-bay steel frame structure. Similarly, more accurate and robust parameter estimations and response predictions are obtained from the adaptive approaches compared to the non-adaptive approach. The results verify the effectiveness and robustness of the proposed adaptive filters. The forgetting factor and moving window methods are shown to have a simpler tuning process compared to the dual adaptive method while providing similar performance.

Keywords: Adaptive Kalman filter; nonlinear model updating; system identification; unscented Kalman filter; modeling errors; covariance-matching technique

1. Introduction

Model updating is the process of tuning structural models using measured data in order to improve the model prediction accuracy. The updated models, especially mechanics-based models, have been shown to be effective for response prediction of dynamic structural systems, structural assessment, and damage identification. The updating process can be performed deterministically through an optimization process or probabilistically through Bayesian inference. Many numerical/laboratory studies and a few of real-world applications of FE model updating through optimization and/or Bayesian inference have been completed with satisfactory results[1-13]. Lam et al. implemented Bayesian model updating of a coupled slab system using modal parameters identified from fast Bayesian FFT method[14, 15]. Behmanesh et al. applied a hierarchical Bayesian framework to study the effect of environmental variability on the uncertainty of model parameters on a footbridge[16] and performed model extrapolation to predict modal parameters at a different structural state for a 10-story building[17]. Song et al. performed damage identification of a two-story reinforced concrete (RC) building through a modeling updating strategy and compared the results with lidar data[18]. In another study, Song et al. implemented hierarchical Bayesian

model updating[19] to account for the amplitude-stiffness nonlinear structural behavior of the same RC building using a linear FE model[20]. Ebrahimian et al. have used an output-only Bayesian finite element (FE) model updating techniques to estimate jointly the soil-structure model parameters and time histories of foundation input motions for the Millikan library building[21].

The response behavior of civil structures is nonlinear in nature due to material and geometric nonlinearities. The nonlinear effects become more significant under larger input loads. Linear dynamic models are only capable of representing civil structures at low amplitudes of vibration. For structures subjected to moderate to large excitations such as seismic loads, nonlinear models should be used for accurate response prediction and structural assessment. The literature includes only few real-world applications of nonlinear model updating. Asgarieh et al. performed nonlinear FE model updating of a large-scale three-story RC frame[22] and a seven-story shear wall[23] tested on shake-table using nonlinear response of the two structures subjected to different earthquake excitations.

Kalman filters (KFs) have received increased attention from the civil engineering community recently for state estimation, parameter estimation, joint state-parameter estimation, and input estimation. KF methods, also referred to as recursive identification methods, can provide certain advantages compared to traditional batch Bayesian model updating method, in which the posterior probability distribution of parameters is updated through a one-step Bayesian inference using the batch of available measurement all at once. Such advantages include (1) the potential for near real-time or near online structural health monitoring through updating structural state/parameter recursively, and (2) the computational efficiency of KF methods compared to batch Bayesian model updating. Several extensions of KFs exist for applications to nonlinear structural systems, such as the extended KF (EKF), the unscented KF (UKF), and particle filters (PFs). Some numerical/laboratory applications of KF have been performed on linear and nonlinear civil structures[24-32]. Wu and Smyth investigated and compared the performance of EKF and UKF for model updating of linear and nonlinear systems[33]. Chatzi and Smyth applied UKF and PF for nonlinear model updating using non-collocated heterogeneous data[34]. Xie and Feng studied the performance of iterated UKF for model updating and compared it with UKF[35]. Ebrahimian et al. implemented EKF for parameter estimation of mechanics-based nonlinear FE model[36] and joint input-parameter estimation[37]. Eftekhar-Azam et al. proposed a dual KF approach for joint state-input estimation using output-only measurements and compared with other existing input estimation methods[38, 39]. Astroza et al. employed UKF for model updating of nonlinear civil structures[40] and seismic input estimation[41], and investigated the effect of modeling errors on parameter estimation[42]. Erazo et al. applied KF for damage assessment of a numerical bridge model and decoupled the effects between structural damage and changing environmental conditions[43]. In another study, Erazo et al. used a UKF for nonlinear model updating and state estimation of a full-scale seven-story shear wall building structure tested on a shake table[44].

Nonlinear KF methods are generally sensitive to the filter parameters and a general approach is lacking for setting the filtering parameters. For example, covariance matrices of process and measurement noises have significant impacts on the filter performance and improper values for these may result in estimation inaccuracy or divergence. In real-world applications, these covariance matrices are usually unknown, and a trial-and-error tuning process is often adopted to determine suitable values for them[45]. Furthermore, modeling errors are unavoidable for large-scale and complex civil structures and have substantial effects on model updating and model predictions. In the presence of significant modeling errors, the measurement noise term, which originally represents the prediction error in KF, can incorporate the effects of modeling errors and its covariance matrix should be considered time-varying since modeling errors often changes with the amplitude of response and the level of response nonlinearity. Poor parameter estimations have been observed using the non-adaptive UKF by Astroza et

al.[42] due to the effects of modeling errors. Several adaptive KF methods exist in the literature that can provide an estimate for the process noise and measurement noise covariance matrices. These methods can be categorized into Bayesian methods, maximum likelihood methods, correlation methods, and covariance-matching methods[46]. Covariance-matching technique is shown to be an effective and easy-to-implement method and has been applied in a few applications in signal processing with reasonable success[47]. Yuen and Kuok proposed an adaptive EKF method using Bayesian method for online estimation of noise covariance[48]. Astroza et al. proposed a dual adaptive UKF to account for the effects of modeling errors for model updating and provided improved parameter estimation results[49]. Almagbile et al. proposed and compared the performance of innovation-based and residual-based covariance-matching techniques for GPS/INS integration[50]. Akhlaghi et al. proposed a forgetting factor adaptive EKF based on residuals for dynamic state estimation[51].

This study proposes adaptive KF methods for nonlinear model updating based on two types of covariance-matching techniques: forgetting factor method and moving window method. Each of the methods is formulated based on innovation as well as residual terms in the KF formulation to estimate the covariance of measurement noise recursively. The forgetting factor and moving window adaptive filters are applied to two numerical applications and their results are compared to those from the non-adaptive UKF and a dual adaptive filter.

2. Adaptive KF for Nonlinear Model Updating

2.1 Non-adaptive KF

The parameter estimation formulation for nonlinear model updating using Kalman-based filters can be written as[36]:

$$\begin{cases} \boldsymbol{\theta}_{k+1} = \boldsymbol{\theta}_k + \mathbf{w}_k & \mathbf{w}_k \sim N(\mathbf{0}, \mathbf{Q}_k) \\ \mathbf{y}_{k+1} = \mathbf{h}_{k+1}(\boldsymbol{\theta}_{k+1}, \mathbf{u}_{1:k+1}) + \mathbf{v}_{k+1} & \mathbf{v}_{k+1} \sim N(\mathbf{0}, \mathbf{R}_{k+1}) \end{cases} \tag{1}$$

in which $\boldsymbol{\theta}_k$ is the vector of updating model parameters, e.g., unknown stiffness, mass, or material constitutive model parameters; $\mathbf{y}_{k+1}$ is the measurement vector at time step k+1, $\mathbf{h}_{k+1}(\boldsymbol{\theta}_{k+1}, \mathbf{u}_{1:k+1})$ refers to the response function of the nonlinear numerical model, e.g., FE model; $\mathbf{u}_{1:k+1}$ is the history of input vector to the system, e.g., earthquake excitation; $\mathbf{w}_k$ and $\mathbf{v}_{k+1}$ are the process and measurement noise vectors with covariance matrices $\mathbf{Q}_k$ and $\mathbf{R}_{k+1}$, respectively. In most applications, $\mathbf{Q}_k$ and $\mathbf{R}_{k+1}$ are taken as constant time-invariable terms. Note that $\mathbf{Q}_k$ and $\mathbf{R}_{k+1}$ are unknown in real-world applications; the selection of these filtering parameters can affect the performance of the filter and may even result in its divergence. For systems with time-invariant parameters, although the covariance of process noise $\mathbf{Q}_k$ can ideally be set as zero, but a small nonzero value of $\mathbf{Q}_k$ is suggested to facilitate faster parameter convergence. Note that the filter may never converge or even diverge if $\mathbf{Q}_k$ is set to zero in applications where the initial state is far from the true value or the initial parameter covariance $\mathbf{P}_0^+$ is not large enough. Therefore, a small nonzero $\mathbf{Q}_k$ is used to improve filter convergence as it is added to the parameter covariance and let the filter better explore the design space.

Modeling errors are inherent part of any numerical model, which should be accounted for to reduce the bias in the estimation results. Here, we assume that the measurement noise term $\mathbf{v}_{k+1}$ can account for

the effects of modeling errors, and, therefore, its covariance $\mathbf{R}_{k+1}$ should be regarded as a time variant variable even when sensor/cable noise is constant. Note that modeling errors can be manifested in the measurement noise term and therefore result in a non-stationary, non-Gaussian, and non-white random process. In this study, we simplify the problem and assume that the modeling errors will result in a non-stationary zero-mean Gaussian measurement noise. This is still a limiting assumption and potentially far from the reality, but a step forward with respect to the state-of-the-art. In this study, adaptive approaches are proposed to estimate the effective values of matrix $\mathbf{R}_{k+1}$ to partially account for the effects of modeling errors. It will be shown later in the paper that by incorporating this assumption, the performance of the Kalman filter will be improved in the presence of modeling errors.

2.2 Covariance-matching technique

The key idea of the covariance-matching method[46] is to update the covariance of $\mathbf{v}_{k+1}$ consistent with the theoretical covariance. Some applications of covariance-matching method have demonstrated its effectiveness in electrical engineering[50, 51] and in civil engineering through a dual filter approach[49]. The concept of covariance matching technique and its derivation are introduced in this section. Note that the following formulation is based on a general state space model, and the parameter estimation formulation in Eq. (1) is just a special nonlinear case/application of it.

Consider the state space model of a linear dynamic system as:

$$\begin{cases} \mathbf{x}_k = \mathbf{A}_{k-1}\mathbf{x}_{k-1} + \mathbf{B}_{k-1}\mathbf{u}_{k-1} + \mathbf{w}_{k-1} & \mathbf{w}_{k-1} \sim N(\mathbf{0}, \mathbf{Q}_{k-1}) \\ \mathbf{y}_k = \mathbf{H}_k\mathbf{x}_k + \mathbf{D}_k\mathbf{u}_k + \mathbf{v}_k & \mathbf{v}_k \sim N(\mathbf{0}, \mathbf{R}_k) \end{cases} \tag{2}$$

where $\mathbf{x}_k$ is the state vector, $\mathbf{A}_{k-1}$ is the state transition matrix, $\mathbf{B}_{k-1}$ is the input matrix, $\mathbf{u}_{k-1}$ is the input vector, $\mathbf{w}_{k-1}$ is the process noise vector, $\mathbf{v}_k$ is the measurement noise vector, $\mathbf{y}_k$ is the observation or measurement vector, $\mathbf{H}_k$ is the observation matrix, and $\mathbf{D}_k$ is the feedthrough matrix. Two covariance-matching formulations are derived (refer to Appendix A and B for derivation details) based on innovation and residual, respectively:

$$\mathbf{R}_k = E\left[\mathbf{d}_k\mathbf{d}_k^T\right] - \mathbf{H}_k\mathbf{P}_k^-\mathbf{H}_k^T \qquad \text{(innovation-based)} \tag{3}$$

$$\mathbf{R}_k = E\left[\boldsymbol{\varepsilon}_k\boldsymbol{\varepsilon}_k^T\right] + \mathbf{H}_k\mathbf{P}_k^+\mathbf{H}_k^T \qquad \text{(residual-based)} \tag{4}$$

in which $\mathbf{d}_k = \mathbf{y}_k - (\mathbf{H}_k\hat{\mathbf{x}}_k^- + \mathbf{D}_k\mathbf{u}_k)$ is the difference between the measurement and its predicted prior response, and is referred as "innovation", and $\boldsymbol{\varepsilon}_k = \mathbf{y}_k - (\mathbf{H}_k\hat{\mathbf{x}}_k^+ + \mathbf{D}_k\mathbf{u}_k)$ is the difference between measurement and the posterior response, and is referred as "residual" in this study. $E\left[\mathbf{d}_k\mathbf{d}_k^T\right]$ denotes the covariance of innovation with E referring to mathematical expectation. $\mathbf{P}_k^-$ and $\mathbf{P}_k^+$ are prior and posterior covariance matrices of response estimation, respectively. In standard KF framework such as linear KF, EKF, and UKF, the term $\mathbf{H}_k\mathbf{P}_k^+\mathbf{H}_k^T$ (or equivalent term in nonlinear KFs) is not calculated in the standard procedure and requires additional calculations, e.g., for UKF, the term $\mathbf{H}_k\mathbf{P}_k^+\mathbf{H}_k^T$ can be approximated using response predictions of all sigma points similar to the calculation of $\mathbf{H}_k\mathbf{P}_k^-\mathbf{H}_k^T$ [52, 53]. For EKF and UKF, these additional computations sometimes are computationally demanding and, therefore, a simplified version of residual-based covariance-matching function is proposed below by replacing the term $\mathbf{H}_k\mathbf{P}_k^+\mathbf{H}_k^T$ with $\mathbf{H}_k\mathbf{P}_k^-\mathbf{H}_k^T$:

$$\mathbf{R}_k = E\left[\boldsymbol{\varepsilon}_k \boldsymbol{\varepsilon}_k^T\right] + \mathbf{H}_k \mathbf{P}_k^- \mathbf{H}_k^T \qquad \text{(residual-based)} \tag{5}$$

Since the estimation uncertainty $\mathbf{P}_k^+$ is usually reduced gradually along the updating time steps (i.e., with increasing k), the difference between $\mathbf{P}_k^+$ and $\mathbf{P}_k^-$ is often small and negligible. The accuracy and efficiency of this simplification have been verified by the authors through a numerical study, and the computational effort is reduced up to 50% when the UKF is applied for model updating.

Based on Eq. (3) and (5), the measurement noise covariance $\mathbf{R}_k$ can be estimated at each updating step using either innovation $\mathbf{d}_k$ or residual $\boldsymbol{\varepsilon}_k$. The only estimation uncertainty comes from evaluating the covariance of innovation $E\left[\mathbf{d}_k \mathbf{d}_k^T\right]$ and residual $E\left[\boldsymbol{\varepsilon}_k \boldsymbol{\varepsilon}_k^T\right]$. Two adaptive methods are proposed in this study using the residual-based formulation, namely the forgetting factor method and the moving window method as outlined in the following sections. Note that the forgetting factor and moving window methods can also be applied using innovation-based formulation in a similar manner as shown in Table 1. For the sake of brevity, only residual-based methods are implemented and investigated in the numerical applications of this study. Some numerical studies have been performed by the authors to compare the performance of residual-based and innovation-based formulations. From these studies, the residual-based formulation was found advantageous since (1) the $\mathbf{R}_k$ estimation is guaranteed to be positive (a lower positive bound is needed for $\mathbf{R}_k$ estimation using innovation-based formulation as it can be estimated as negative in certain cases), and (2) the full covariance matrix is obtained (only diagonal entries are estimated using innovation-based methods), whose off-diagonal entries contain information about the noise correlation and modeling errors correlation.

2.2.1 Forgetting factor method

Forgetting factor method is first proposed by Akhlaghi et al. for dynamic state estimation in electrical system[51]. The basic idea of this method is to update $\mathbf{R}_k$ gradually according to current residual values by applying a forgetting factor α to balance the weight between previous covariance $\mathbf{R}_{k-1}$ and the current residual estimation term, i.e.,

$$\mathbf{R}_k = \alpha \mathbf{R}_{k-1} + (1-\alpha)\left(\boldsymbol{\varepsilon}_k \boldsymbol{\varepsilon}_k^T + \mathbf{H}_k \mathbf{P}_k^- \mathbf{H}_k^T\right) \qquad (0 \le \alpha \le 1) \tag{6}$$

In Eq. (6), if $\alpha = 1$, the forgetting factor method would become the traditional non-adaptive filtering method, in which $\mathbf{R}_k$ is not updated and treated as a constant. If $\alpha = 0$, then $\mathbf{R}_k$ is fully determined by current residual term, which usually should be avoided as this causes too much variation in the estimation of $\mathbf{R}_k$. Generally larger values of α would assign larger weights to previous $\mathbf{R}_{k-1}$ and, therefore, estimated $\mathbf{R}_k$ will change slower and smoother.

2.2.2 Moving window method

The covariance of residual $E\left[\boldsymbol{\varepsilon}_k \boldsymbol{\varepsilon}_k^T\right]$ in Eq. (5) can be approximated within a moving window as proposed by Mehra[46] and employed by Almagbile et al[50]. In this way, the moving window method is formulated as

$$\mathbf{R}_k = \frac{1}{m} \sum_{i=0}^{m-1} \boldsymbol{\varepsilon}_{k-i} \boldsymbol{\varepsilon}_{k-i}^T + \mathbf{H}_k \mathbf{P}_k^- \mathbf{H}_k^T \tag{7}$$

In Eq. (7), m refers to the size of the moving window. A larger window size would provide statistical smoothing so that updated $\mathbf{R}_k$ changes smoother and slower. For model updating at the beginning of time history (i.e., when $k < m$), two strategies can be employed: (1) keep $\mathbf{R}_k$ fixed as the initial $\mathbf{R}_0$ and start updating $\mathbf{R}_k$ once k reaches window size m; (2) start updating $\mathbf{R}_k$ from a specific time step L ($L \le m$) and for $L \le k \le m$, the sample mean term in Eq. (7) is estimated over available residual values $\boldsymbol{\varepsilon}_1 \sim \boldsymbol{\varepsilon}_k$. In this study, the second strategy is adopted with $L = 5$.

2.2.3 Dual adaptive UKF

A dual adaptive UKF is proposed by Astroza et al.[49] to update $\mathbf{R}_k$ and account for the effects of modeling errors for nonlinear FE model updating. The basic idea of this method is to build a slave linear KF to update $\mathbf{R}_k$ recursively embedded in a master UKF for model updating. For the slave KF, the diagonal terms of $\mathbf{R}_k$ are treated as unknown parameters and the innovation-based covariance-matching function Eq. (3) is used as measurement function. More details about this method can be found in Table 1 and in[49].

2.3 Adaptive UKF for nonlinear model updating

A step-by-step flowchart for the proposed adaptive UKF approaches including the forgetting factor, moving window, and dual adaptive methods is provided in Table 1. Innovation-based forgetting factor and moving window methods are also included (although not implemented in the application studies of this paper) to provide a complete demonstration of covariance-matching-based adaptive approaches. The framework for non-adaptive UKF can be obtained from Table 1 by not implementing the adaptive sections. Note that only one of the two adaptive options is needed for adaptive UKF. As previously mentioned, the proposed innovation-based and residual-based methods can alternatively be combined with other nonlinear KFs such as EKF and EnKF.

The residual-based adaptive methods have the following two advantages over the innovation-based methods: (1) full matrix $\mathbf{R}_k$ can be estimated and the off-diagonal terms contain information about noise/modeling error correlation, while for innovation-based approaches only diagonal terms of $\mathbf{R}_k$ are updated to simplify the problem and avoid ill-conditioning, and (2) $\mathbf{R}_k$ is guaranteed to be positive definite since it is estimated to be the summation of two positive definite terms, but the positive definiteness of $\mathbf{R}_k$ in innovation-based methods is not guaranteed and a small positive lower bound has to be assigned to avoid computational errors. Furthermore, there is only one tuning parameter for the forgetting factor method (forgetting factor α) and moving window method (window size m) compared to at least two tuning matrices $\mathbf{T}$ and $\mathbf{U}$ for the dual adaptive method, in which $\mathbf{T}$ is the covariance matrix of process noise and $\mathbf{U}$ is the covariance matrix of measurement noise for the slave linear KF. It is worth noting that $\mathbf{T}$ and $\mathbf{U}$ are symmetric covariance matrices of size $n_y \times n_y$ (n_y is the measurement size) and, therefore, can have up to $n_y(n_y+1)/2$ independent variables each. In practice, both $\mathbf{T}$ and $\mathbf{U}$ are assumed to be diagonal matrices with a single independent diagonal element each, namely σ_T^2 for $\mathbf{T}$ and σ_U^2 for $\mathbf{U}$. However, since parameters α and m are scalars and their effects on the filter performance are better understood, the selection of these parameters in forgetting factor and moving window methods is easier and more straightforward than the tuning procedure of slave KF for dual adaptive method.

The estimated $\mathbf{R}_k$ from the adaptive approaches reflects the "effective noise covariance matrix" that also accounts for modeling errors. Larger values for innovation or residual means larger discrepancy between measurement and model prediction, which would increase $\mathbf{R}_k$ and, therefore, reduce the Kalman gain (step (2.3) in Table 1). Lower Kalman gain assigns smaller weight on the measurements (step (2.4) in Table 1) in the KF correction step and, therefore, the correction in $\hat{\boldsymbol{\theta}}_{k+1}^{+}$ becomes smaller and the reduction in $\mathbf{P}_{k+1}^{+}$ (step (2.5) in Table 1) also becomes smaller. This means that the filter becomes less sensitive to the discrepancies between the measurement and model prediction and assumes that the discrepancies stem from potential modeling errors rather than model parameter uncertainties.

The parameters used in Table 1 are defined as follows[52, 53]. At step (1.2), $\gamma = \sqrt{n_\theta + \lambda}$ in which n_θ is the dimension of $\boldsymbol{\theta}$ and $\lambda = \alpha^2(n_\theta + \kappa) - n_\theta$ is a scaling parameter, κ is a secondary scaling parameter which is usually set to 0 or $3 - n_\theta$, and α determines the spread of sigma points (SP) and is usually set to a small positive value $1e-4 \le \alpha \le 1$. At steps (1.4), (a.2), (2.1), (2.2) and (b.3), the weights $W_m^{(i)}$ and $W_c^{(i)}$ are determined as

$$W_m^{(1)} = \lambda/(n_\theta + \lambda), \quad W_c^{(1)} = \lambda/(n_\theta + \lambda) + (1 - \alpha^2 + \beta) \tag{8}$$

$$W_m^{(i)} = W_c^{(i)} = 0.5/(n_\theta + \lambda) \qquad i = 2, \ldots, 2n_\theta + 1 \tag{9}$$

In this study, the parameter values are selected as: $\kappa = 0$, $\alpha = 1$, and $\beta = 2$.

Table 1. Framework of adaptive UKF approaches

Initialize: $\hat{\boldsymbol{\theta}}_0^{+}$, $\mathbf{P}_0^{+}$

Loops for k = 0, 1, 2, 3…N-1

UKF Step 1: Prediction Step

(1.1) $\hat{\boldsymbol{\theta}}_{k+1}^{-} = \hat{\boldsymbol{\theta}}_k^{+}$, $\mathbf{P}_{k+1}^{-} = \mathbf{P}_k^{+} + \mathbf{Q}_k$

(1.2) Generate sigma points (SP): $\boldsymbol{\Theta}_{k+1|k} = \left[\hat{\boldsymbol{\theta}}_{k+1}^{-} \quad \hat{\boldsymbol{\theta}}_{k+1}^{-} + \gamma\sqrt{\mathbf{P}_{k+1}^{-}} \quad \hat{\boldsymbol{\theta}}_{k+1}^{-} - \gamma\sqrt{\mathbf{P}_{k+1}^{-}}\right]$

(1.3) Evaluate predictions at SP: $\boldsymbol{\mathcal{Y}}_{k+1|k} = \mathbf{h}_{k+1}\left(\boldsymbol{\Theta}_{k+1|k}, \ddot{\mathbf{u}}_{1:k+1}\right)$

(1.4) Mean of prediction: $\hat{\mathbf{y}}_{k+1}^{-} = \sum_{i=1}^{2n_\theta+1} W_m^{(i)} \boldsymbol{\mathcal{Y}}_{k+1|k}^{(i)}$

Adaptive Option a: Innovation-based Covariance-matching Methods

(a.1) Evaluate innovation: $\mathbf{d}_{k+1} = \mathbf{y}_{k+1} - \hat{\mathbf{y}}_{k+1}^{-}$

(a.2) Based on covariance-matching equation $\mathbf{R}_{k+1} = E\left[\mathbf{d}_{k+1}\mathbf{d}_{k+1}^T\right] - \mathbf{H}_{k+1}\mathbf{P}_{k+1}^{-}\mathbf{H}_{k+1}^T$, three adaptive methods can be applied:

Forgetting factor method: $\mathbf{r}_{k+1} = \alpha\mathbf{r}_k + (1-\alpha)diag\left(\mathbf{d}_{k+1}\mathbf{d}_{k+1}^T - \mathbf{l}_{k+1}\right)$

Moving window method: $\mathbf{r}_{k+1} = diag\left(\frac{1}{m}\sum_{i=0}^{m-1}\mathbf{d}_{k+1-i}\mathbf{d}_{k+1-i}^T - \mathbf{l}_{k+1}\right)$

Dual adaptive UKF: $\begin{cases}\mathbf{r}_{k+1} = \mathbf{r}_k + \boldsymbol{\omega}_k & \boldsymbol{\omega}_k \sim N(\mathbf{0}, \mathbf{T}) \\ diag\left(\mathbf{d}_{k+1}\mathbf{d}_{k+1}^T\right) = \mathbf{r}_{k+1} + \mathbf{l}_{k+1} + \boldsymbol{\upsilon}_{k+1} & \boldsymbol{\upsilon}_{k+1} \sim N(\mathbf{0}, \mathbf{U})\end{cases}$

where $\mathbf{r}_{k+1} = diag\left(\mathbf{R}_{k+1}\right)$ and $\mathbf{l}_{k+1} = diag\left(\sum_{i=1}^{2n_\theta+1} W_c^{(i)}\left[\boldsymbol{\mathcal{Y}}_{k+1|k}^{(i)} - \hat{\mathbf{y}}_{k+1}^{-}\right]\left[\boldsymbol{\mathcal{Y}}_{k+1|k}^{(i)} - \hat{\mathbf{y}}_{k+1}^{-}\right]^T\right)$

UKF Step 2: Correction Step

(2.1) $\mathbf{P}_{\mathbf{y}_{k+1}\mathbf{y}_{k+1}} = \sum_{i=1}^{2n_\theta+1} W_c^{(i)}\left[\boldsymbol{\mathcal{Y}}_{k+1|k}^{(i)} - \hat{\mathbf{y}}_{k+1}^{-}\right]\left[\boldsymbol{\mathcal{Y}}_{k+1|k}^{(i)} - \hat{\mathbf{y}}_{k+1}^{-}\right]^T + \mathbf{R}_{k+1}$ (For innovation-based methods, estimated $\mathbf{R}_{k+1}$ from step (a.2) will be directly used here; for residual-based methods, $\mathbf{R}_{k+1}$ estimated from step (b.3) in previous loop *k* is used here)

(2.2) $\mathbf{P}_{\boldsymbol{\theta}_{k+1}\mathbf{y}_{k+1}} = \sum_{i=1}^{2n_\theta+1} W_c^{(i)}\left[\boldsymbol{\Theta}_{k+1|k} - \hat{\boldsymbol{\theta}}_{k+1}^{-}\right]\left[\boldsymbol{\mathcal{Y}}_{k+1|k}^{(i)} - \hat{\mathbf{y}}_{k+1}^{-}\right]^T$

(2.3) Kalman gain: $\mathbf{K}_{k+1} = \mathbf{P}_{\boldsymbol{\theta}_{k+1}\mathbf{y}_{k+1}}\left(\mathbf{P}_{\mathbf{y}_{k+1}\mathbf{y}_{k+1}}\right)^{-1}$

(2.4) Parameter update: $\hat{\boldsymbol{\theta}}_{k+1}^{+} = \hat{\boldsymbol{\theta}}_{k+1}^{-} + \mathbf{K}_{k+1}\left(\mathbf{y}_{k+1} - \hat{\mathbf{y}}_{k+1}^{-}\right)$

(2.5) Parameter uncertainty update: $\mathbf{P}_{k+1}^{+} = \mathbf{P}_{k+1}^{-} - \mathbf{K}_{k+1}\mathbf{P}_{\mathbf{y}_{k+1}\mathbf{y}_{k+1}}\mathbf{K}_{k+1}^T$

Adaptive Option b: Residual-based Covariance-matching Methods

(b.1) Evaluate updated prediction: $\hat{\mathbf{y}}_{k+1}^{+} = \mathbf{h}_{k+1}\left(\hat{\boldsymbol{\theta}}_{k+1}^{+}, \ddot{\mathbf{u}}_{1:k+1}\right)$

(b.2) Evaluate residual: $\boldsymbol{\varepsilon}_{k+1} = \mathbf{y}_{k+1} - \hat{\mathbf{y}}_{k+1}^{+}$

(b.3) Update $\mathbf{R}_{k+1}$ which is used for next loop *k*+2 in step (2.1):

Forgetting factor method: $\mathbf{R}_{k+1} = \alpha\mathbf{R}_k + (1-\alpha)\left(\boldsymbol{\varepsilon}_{k+1}\boldsymbol{\varepsilon}_{k+1}^T + \mathbf{L}_{k+1}\right)$

Moving window method: $\mathbf{R}_{k+1} = \frac{1}{m}\sum_{i=0}^{m-1}\boldsymbol{\varepsilon}_{k+1-i}\boldsymbol{\varepsilon}_{k+1-i}^T + \mathbf{L}_{k+1}$

where $\mathbf{L}_{k+1} = \sum_{i=1}^{2n_\theta+1} W_c^{(i)}\left[\boldsymbol{\mathcal{Y}}_{k+1|k}^{(i)} - \hat{\mathbf{y}}_{k+1}^{-}\right]\left[\boldsymbol{\mathcal{Y}}_{k+1|k}^{(i)} - \hat{\mathbf{y}}_{k+1}^{-}\right]^T$

End loop for *k*

3. Application 1: Cantilever Steel Pier

3.1 FE model and numerical simulation

In the first application study, the proposed adaptive KF approaches are applied to a nonlinear cantilever steel pier with a concentrated mass at the top. The FE model of the cantilever pier is created in open-source FE analysis platform OpenSees[54] as shown in Figure 1(a). The pier column is modeled using displacement-based beam-column elements considering P-Delta effect. The column is discretized into 17 elements where the 10 bottom elements are 250 mm long and the 7 top elements are 500 mm long. The steel box section of the column is modeled using fiber elements with the Giuffre-Menegotto-Pinto (GMP)[55] constitutive model characterizing the uniaxial behavior of the steel fibers as shown in Figure 1(b). The model includes stiffness proportional Rayleigh damping with 2% damping at the first mode. Three parameters of the GMP model are selected as updating parameters, namely the initial Young's modulus *E*, yielding stress f_y, and strain-hardening ratio *b*. The nominal values of these parameters, referred to as the true values in this paper, are taken as: $E^{\text{true}} = 200$ GPa , $f_y^{\text{true}} = 250$ MPa ,

$b^{\text{true}} = 0.08$. In the estimation process, the updating parameters are normalized by their true values, i.e., $\boldsymbol{\theta} = \left[E / E^{\text{true}} \quad f_y / f_y^{\text{true}} \quad b / b^{\text{true}} \right]^T$.

The measurement data consists of the absolute acceleration response at the top of the pier subjected to the 1989 Loma Prieta earthquake (0° component at Los Gatos station[56]) as shown in Figure 2. The simulated acceleration response is then polluted with additive white noise of 10% root-mean-square (RMS) noise-signal-ratio (NSR), i.e., $\text{RMS(noise)} = 0.1 \times \text{RMS}(y^{\text{true}})$ in which y^{true} refers to simulated acceleration response at the top of pier without noise. Therefore, the true covariance of measurement noise $R^{\text{true}} = 0.01 \times \text{RMS}(y^{\text{true}})^2$. Note that 10% RMS NSR noise level is significantly higher than common expected measurement noise level in real-world applications, and the purpose of this numerical study is to demonstrate the effectiveness of adaptive approaches to estimate *R* when the initial value is far from the true value which is clearly known. Furthermore, 10% NSR noise can represent the effects of small modeling errors. It has been shown that, if the top mass is 5% larger than the original value (100 t), the top acceleration discrepancy is 11% of the true response when evaluated as RMS, i.e., $\text{RMS}(y^{\text{true}} - y^{\text{error}}) / \text{RMS}(y^{\text{true}}) = 11\%$ where y^{error} refers to the response of model with 5% larger top mass than the true model. Therefore, the case study in Application 1 can also be seen as model updating with the existence of modeling errors.

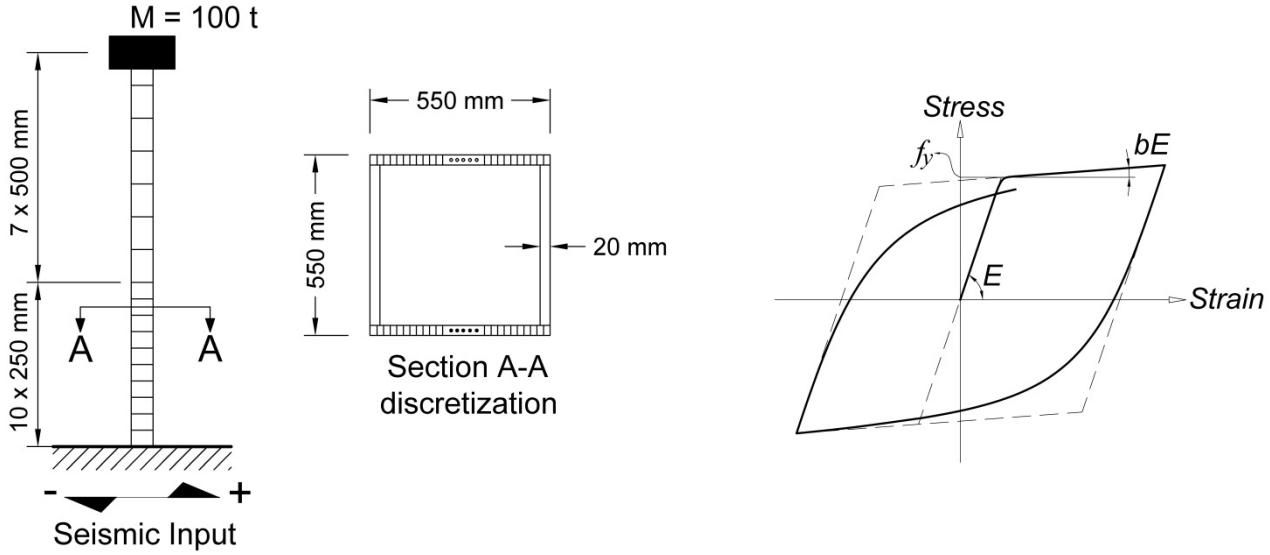

(a) (b)

Figure 1. (a) FE model of cantilever steel pier; (b) Giuffre-Menegotto-Pinto material model

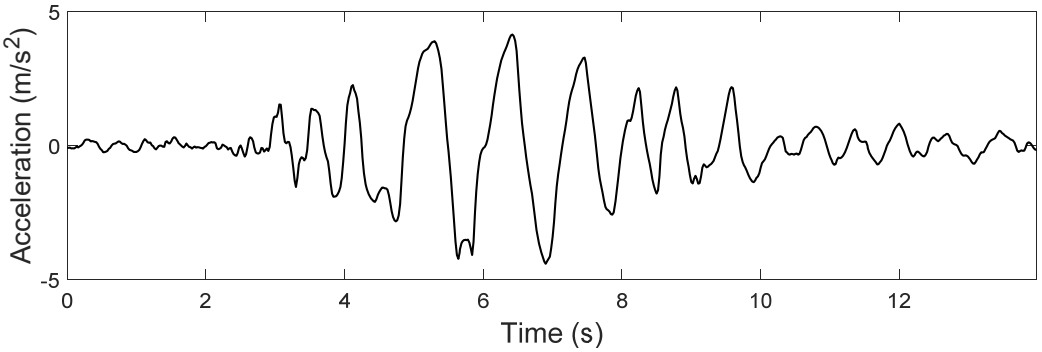

Figure 2. 1989 Loma Prieta earthquake recorded in the 0° component at Los Gatos station

3.2 Model updating results

The non-adaptive UKF and the three adaptive UKF approaches (forgetting factor, moving window and dual adaptive methods) are applied to estimate the model parameter vector $\boldsymbol{\theta}$ of the cantilever steel pier. The initial parameter values of $\hat{\boldsymbol{\theta}}_0^+ = \begin{bmatrix} 0.7 & 0.7 & 1.5 \end{bmatrix}^T$ and the initial parameter covariance matrix $\mathbf{P}_0^+ = diag\left(0.2\hat{\boldsymbol{\theta}}_0^+\right)^2$ are considered. The process noise covariance is taken as $\mathbf{Q} = diag\left(10^{-4}\hat{\boldsymbol{\theta}}_0^+\right)^2$. Figure 3 shows the estimated parameters from the non-adaptive approach. Two cases of model updating are investigated when using the non-adaptive method, with $R = R^{\text{true}}$ and $R = R^{\text{true}}/100$ (i.e., 1% RMS NSR). It can be observed that accurate parameter estimations are obtained when R^{true} is used, while the estimated parameters do not converge to the true values when R is underestimated, especially for strain-hardening ratio b which is the least sensitive parameter to the measured data. It is worth noting that different assumptions for initial R could be used, for example $R = R^{\text{true}}/N$, with $N = 2$, or 10. However, $N = 100$ is selected to clearly show the performance of adaptive approaches under an extreme condition. Note that for $N = 2$ or 10, model updating results of adaptive approaches will be improved.

The three adaptive approaches are applied with initial $R = R^{\text{true}}/100$ for fair comparison. The time histories of parameter estimation and the estimation uncertainties (shown as standard deviations, which are obtained from the diagonal entries of the covariance matrix **P**) using the forgetting factor method are shown in Figure 4 with four factor values of α = 0.5, 0.7, 0.9 and 0.95. It can be seen that the forgetting factor method with all four different factor values improves the model updating results remarkably, and the estimated parameters and their uncertainties are similar to the non-adaptive approach with R^{true}, which can be regarded as the reference results. The estimated R from the forgetting factor method is plotted in Figure 5. It can be observed that the estimated R changes drastically starting from initial R and reach R^{true} quickly, and then fluctuates around it. As expected, larger α values reduce the estimation uncertainty and provide smoother results. Overall, R estimations are acceptable and better approximations are obtained when average of R over a window is used.

Moving window method is applied with four different window sizes of m = 5, 10, 20 and 40. Estimated parameters and their standard deviations are shown in Figure 6. Similar observations can be made to those of the forgetting factor method: parameters are estimated accurately with standard deviations comparable with reference results. Larger window sizes provide statistical smoothing in the R estimation as shown in Figure 7, similar to the effect of factor α. Model updating results using dual adaptive method with four different settings (U = 1e-20, 1e-19, 1e-18 and 1e-17 where 1e-20 was used in the original study of dual adaptive filer[49]) are shown in Figure 8. Note that there are two tuning parameters for dual adaptive method: T and U; however, as there is compensation effect between them, it is suggested to tune only one of them. In this study, T is fixed as 1e-20 and the effect of U is studied. Overall, the estimated parameters and standard deviations are improved, and the results are comparable with forgetting factor and moving window approaches. It is worth noting that for U = 1e-20, small estimation errors are observed which is due to the large variability of R estimation as shown in Figure 9. The effect of U is similar to that of factor α and window size m, with larger U providing statistical smoothing in R estimation as shown in Figure 9.

The comparison between the non-adaptive and three adaptive methods is shown in Figure 10. It can be seen that the three adaptive methods (forgetting factor method with α = 0.9, moving window method with m = 20, and dual adaptive method with U = 1e-18) provide similar parameter estimation and standard deviations which have been significantly improved compared to non-adaptive method when the same initial $R = R^{\text{true}}/100$ is used. The parameter uncertainty from non-adaptive method with

$R^{\text{true}}/100$ used is drastically smaller than that of the reference filter and adaptive methods, which would provide un-conservative parameter confidence interval. The comparison of R estimation across different methods is shown in Figure 11. It is interesting to observe that three adaptive methods provide almost the same R estimation along the time history, especially between forgetting factor and dual adaptive method which almost overlay each other. This shows that three adaptive methods, although formulated differently based on different philosophy and covariance-matching functions, provide similar performance on parameter and R estimation. Overall, this case study demonstrates the robustness of adaptive methods for parameter estimation and the effectiveness of R estimation.

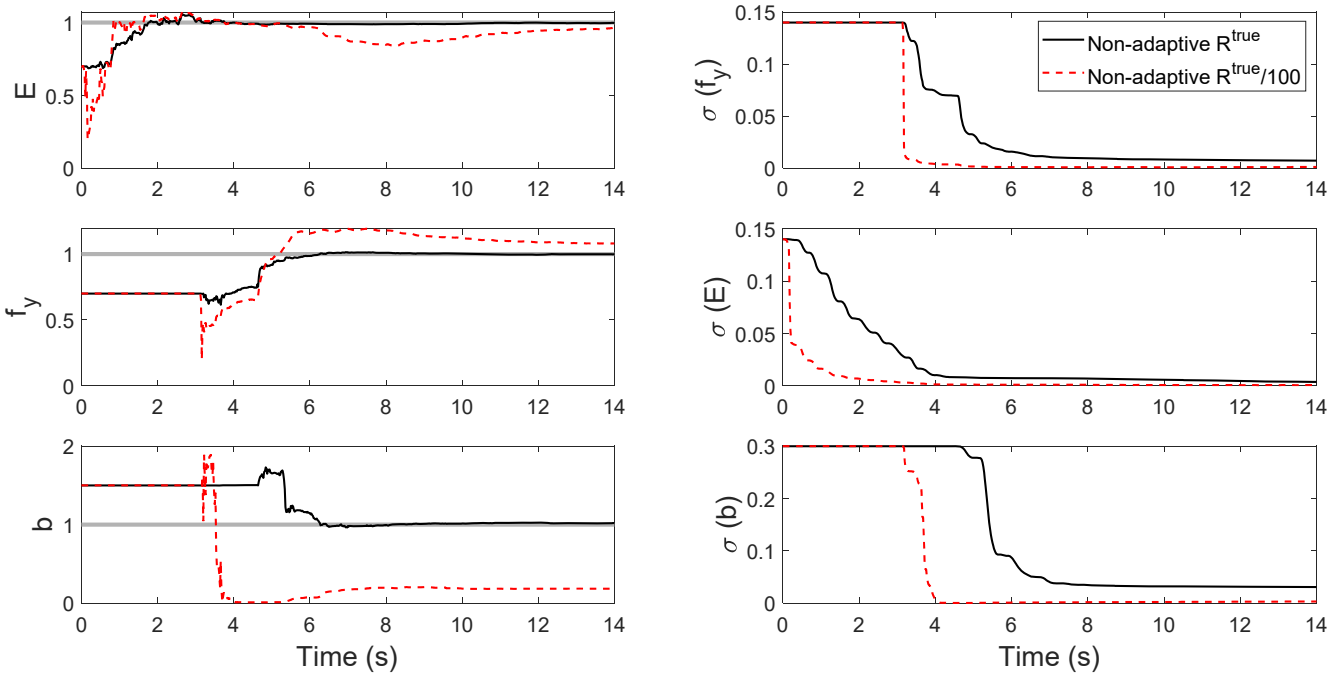

Figure 3. Parameter and standard deviation estimation histories using non-adaptive approach with R^{true} and $R^{\text{true}}/100$ used

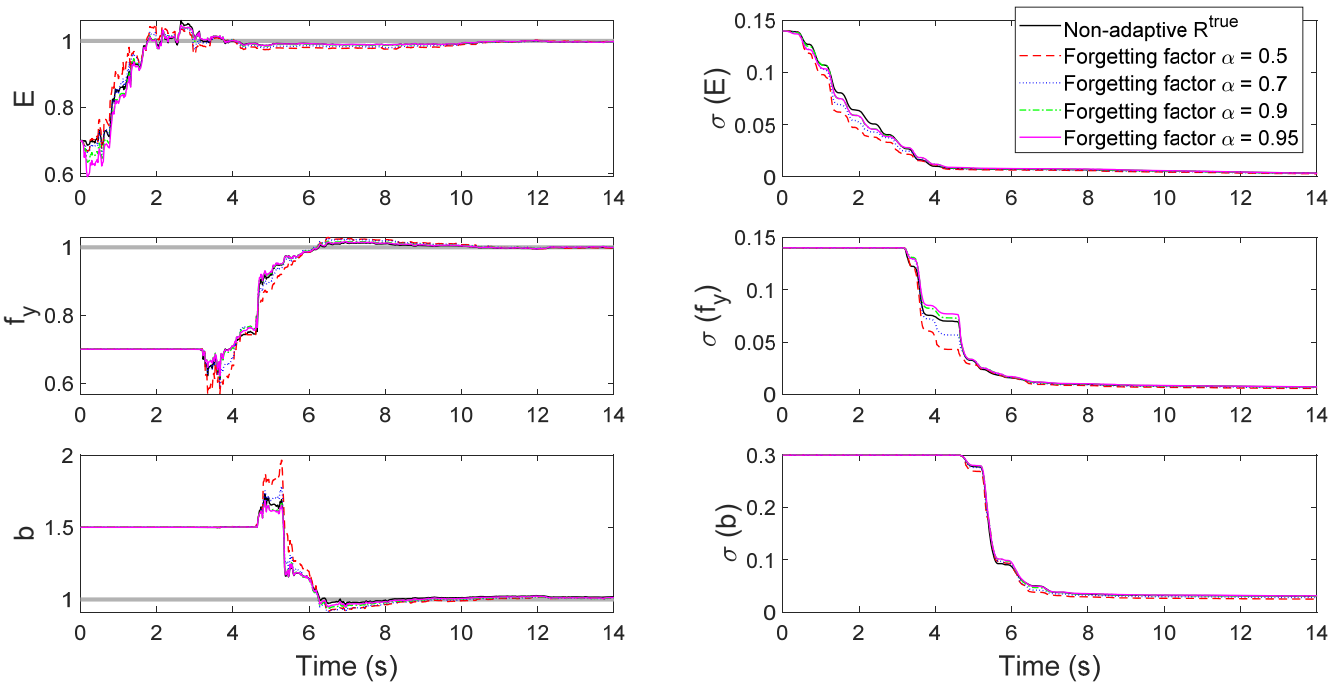

Figure 4. Parameter and standard deviation estimation histories using forgetting factor approach with α = 0.5, 0.7, 0.9, and 0.95

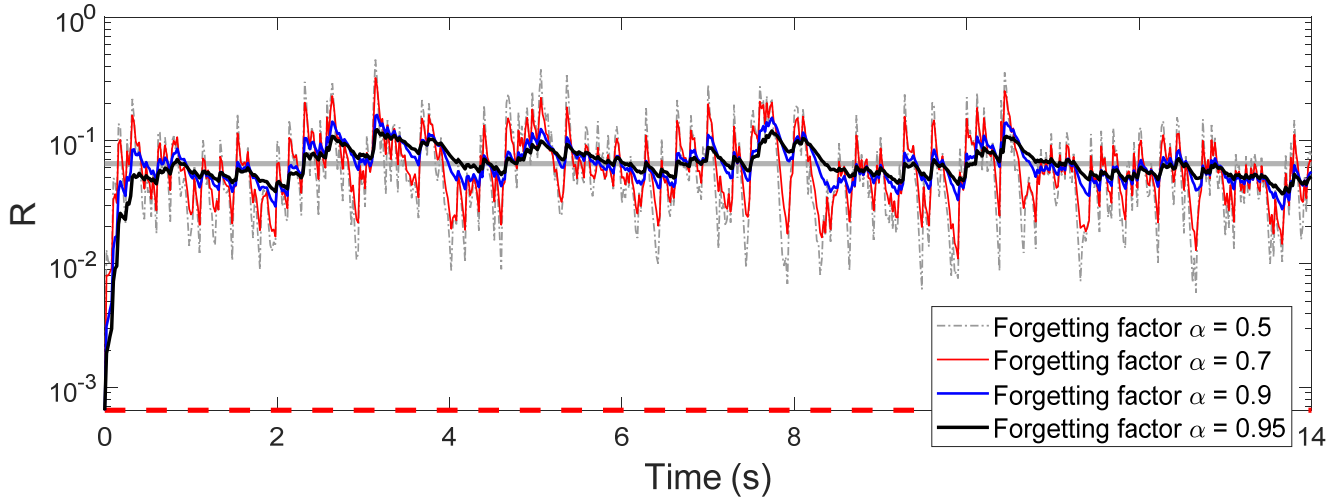

Figure 5. Covariance R estimation histories using forgetting factor approach with α = 0.5, 0.7, 0.9, and 0.95 (R^{true} and $R^{\text{true}}/100$ are denoted by horizontal solid and dash lines respectively)

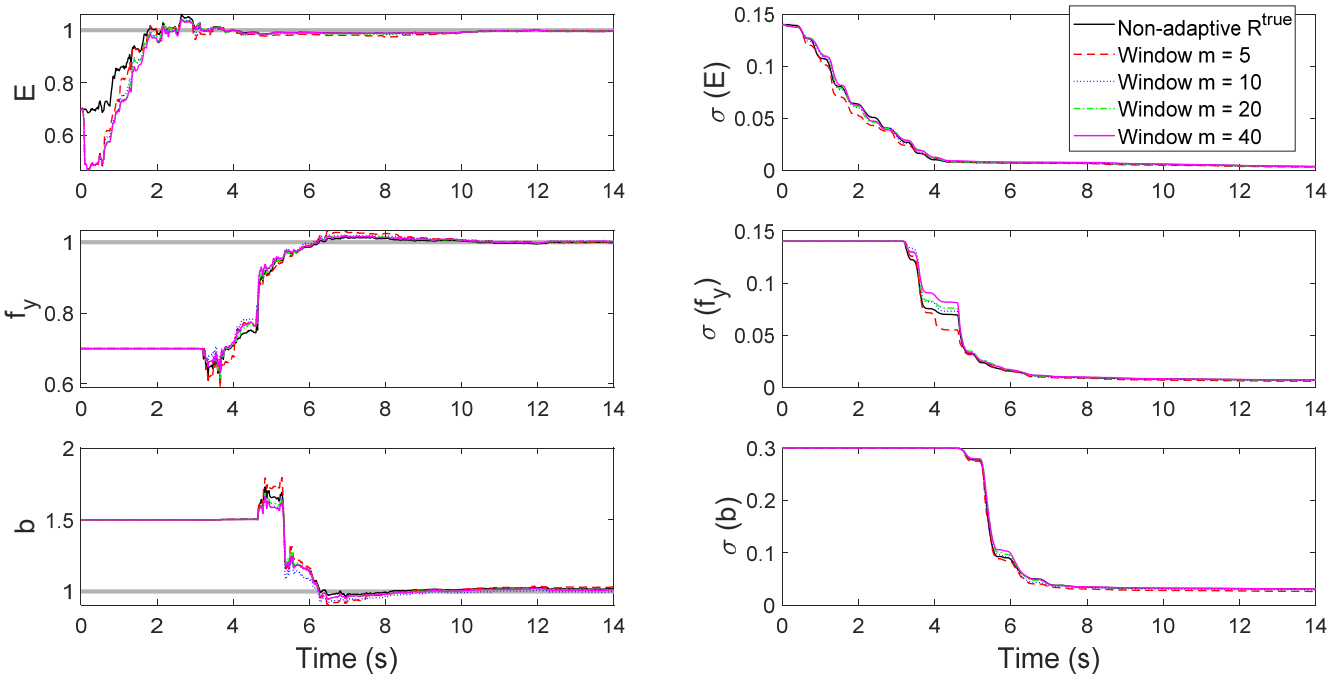

Figure 6. Parameter and standard deviation estimation histories using moving window approach with *m* = 5, 10, 20, and 40

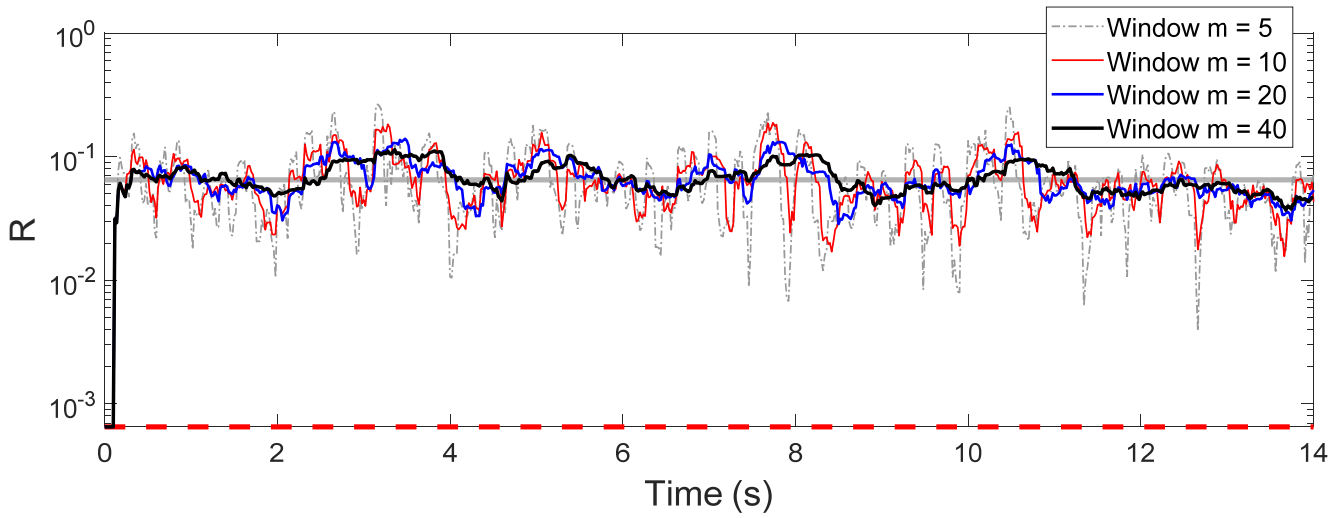

Figure 7. Covariance R estimation histories using moving window approach with *m* = 5, 10, 20, and 40 (R^{true} and $R^{true}/100$ are denoted by horizontal solid and dash lines respectively)

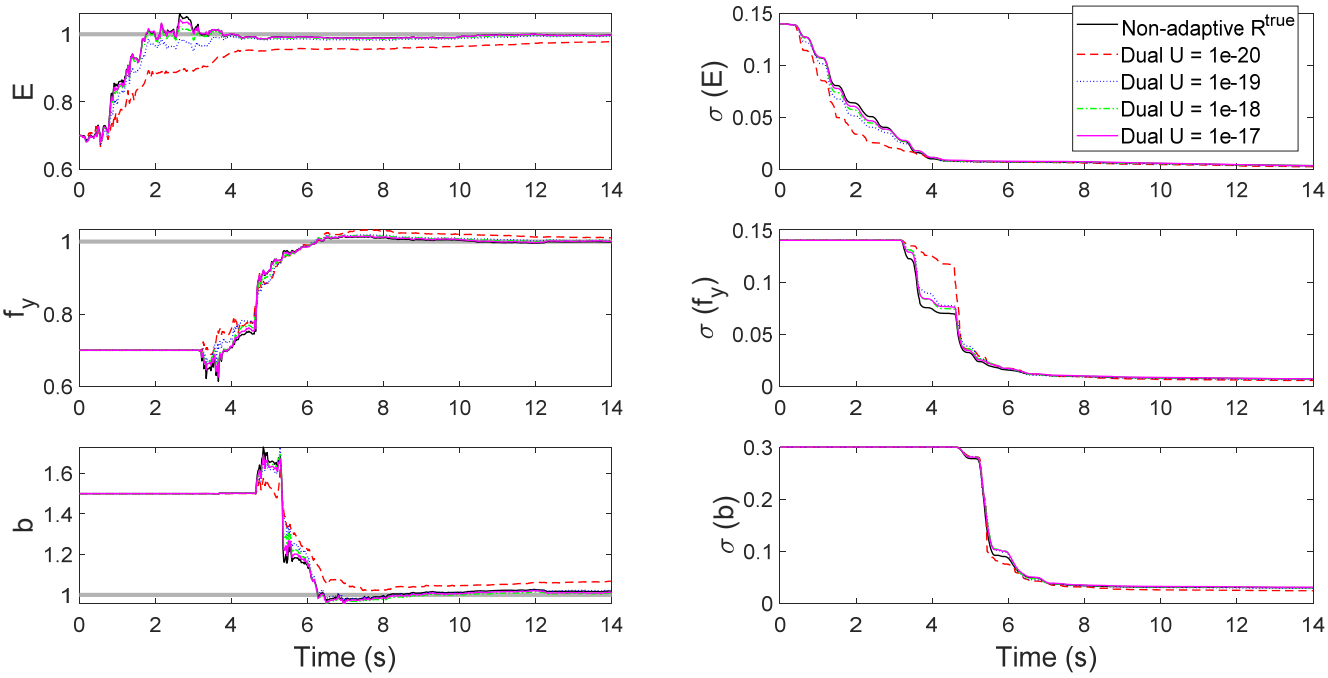

Figure 8. Parameter and standard deviation estimation histories using dual adaptive approach with U = 1e-20, 1e-19, 1e-18 and 1e-17

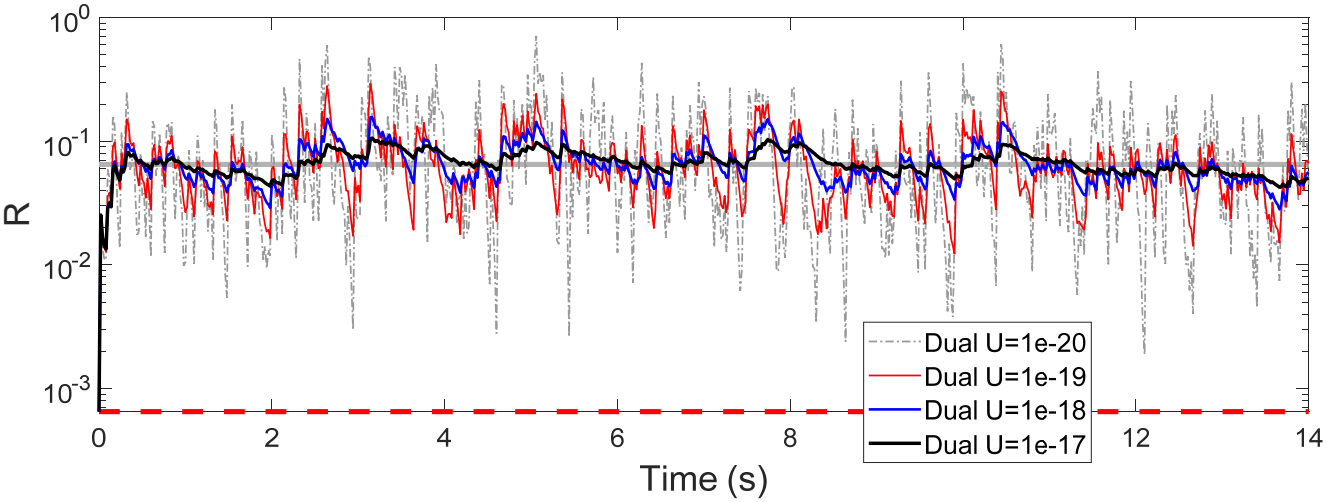

Figure 9. Covariance R estimation histories using dual adaptive approach with U = 1e-20, 1e-19, 1e-18 and 1e-17 (R^{true} and $R^{\text{true}}/100$ are denoted by horizontal solid and dash lines respectively)

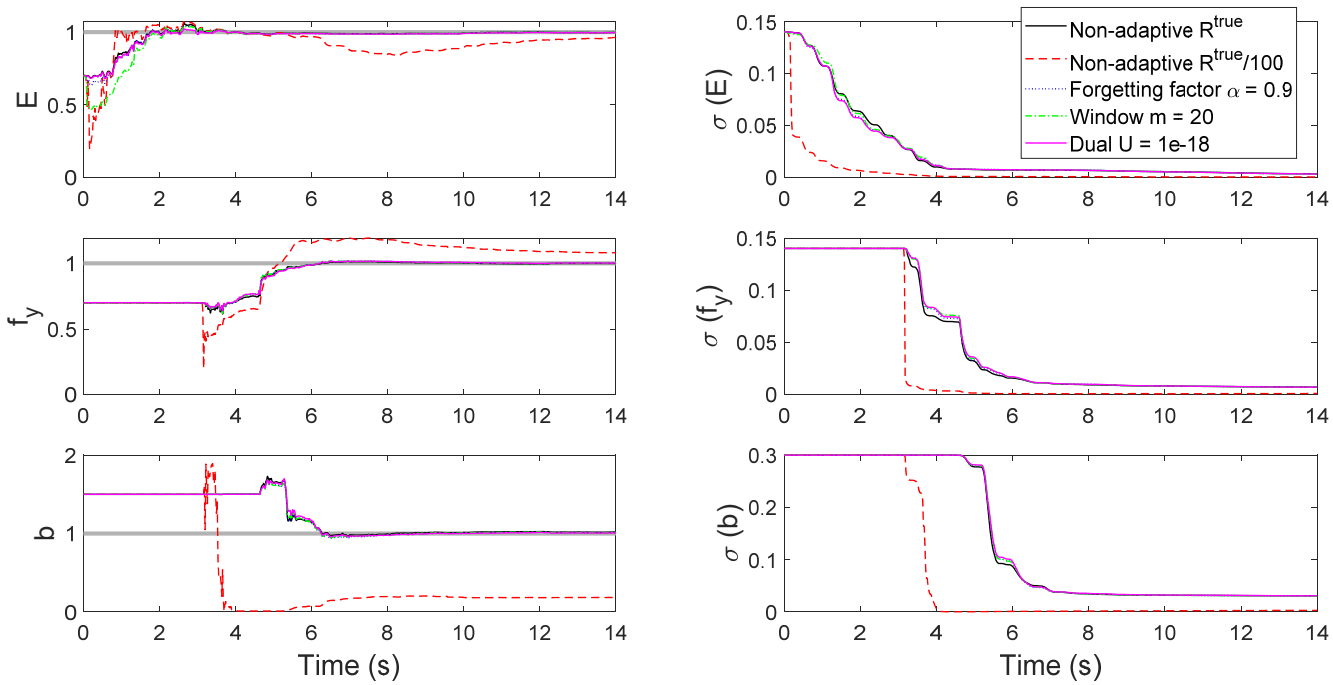

Figure 10. Comparison of parameter estimation and standard deviation between non-adaptive and adaptive methods

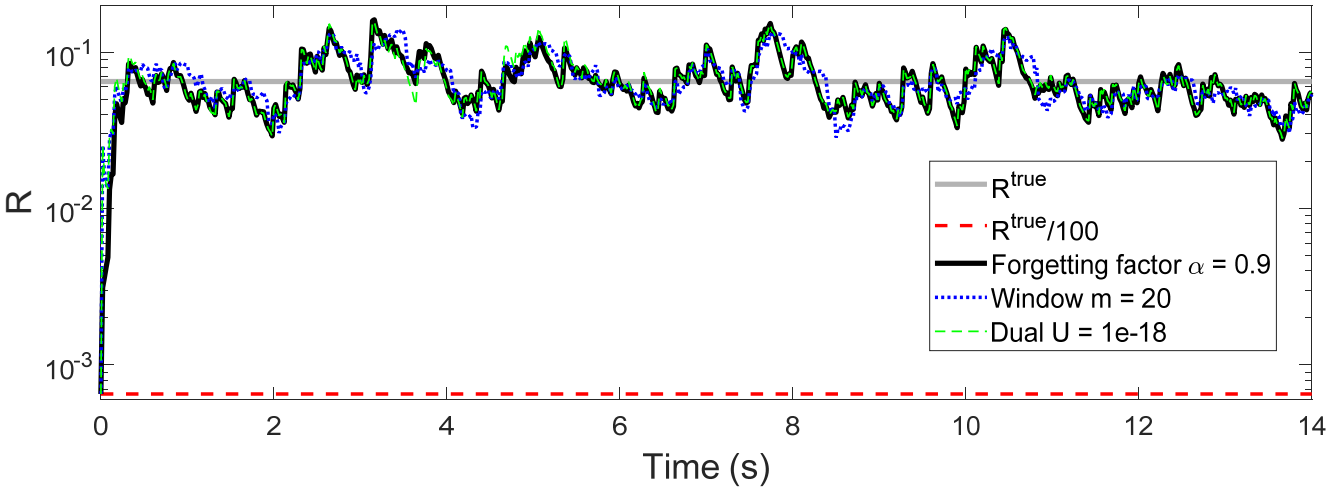

Figure 11. Comparison of R estimation among three adaptive methods

4. Application 2: 3-story 3-bay Steel Frame

4.1 FE model and simulations

The second numerical application considers the effect of modeling errors on model updating of a 3-story 3-bay steel moment resisting frame known as SAC-LA3[57], which is shown in Figure 12. The FE model of this structure is created in OpenSees[54]. The measurement data is simulated using the same 1989 Loma Prieta earthquake records used in previous example (Figure 2). Horizontal absolute acceleration responses are measured at three floors at locations denoted by black boxes in Figure 12. The simulated acceleration responses are then polluted with additive 1% RMS NSR Gaussian white

noise, i.e., $\text{RMS(noise)} = 0.01 \times \text{RMS}(y^{\text{true}})$ independently for each of the three channels. Therefore, the true covariance of measurement noise $\mathbf{R}^{\text{noise}} = 10^{-4} \times diag\left(\text{RMS}(\mathbf{y}^{\text{true}})\right)^2$ in which $\mathbf{y}^{\text{true}}$ consists of three channels y_1^{true}, y_2^{true}, and y_3^{true}. Force-based beam-column elements are used to model columns and beams with 6 and 7 integration points, respectively. The columns and beams consist of different wide flange sections as shown in Figure 12. Structural damping is assumed to be Rayleigh damping with 2% damping coefficients for the first two modes. Finite element masses are assumed to be concentrated at nodes and each story is subjected to the uniformly distributed gravity loads displayed in Figure 12. The constitutive model of steel material is the GMP model and the true (nominal values used in simulation) material properties for columns and beams are reported in Table 2.

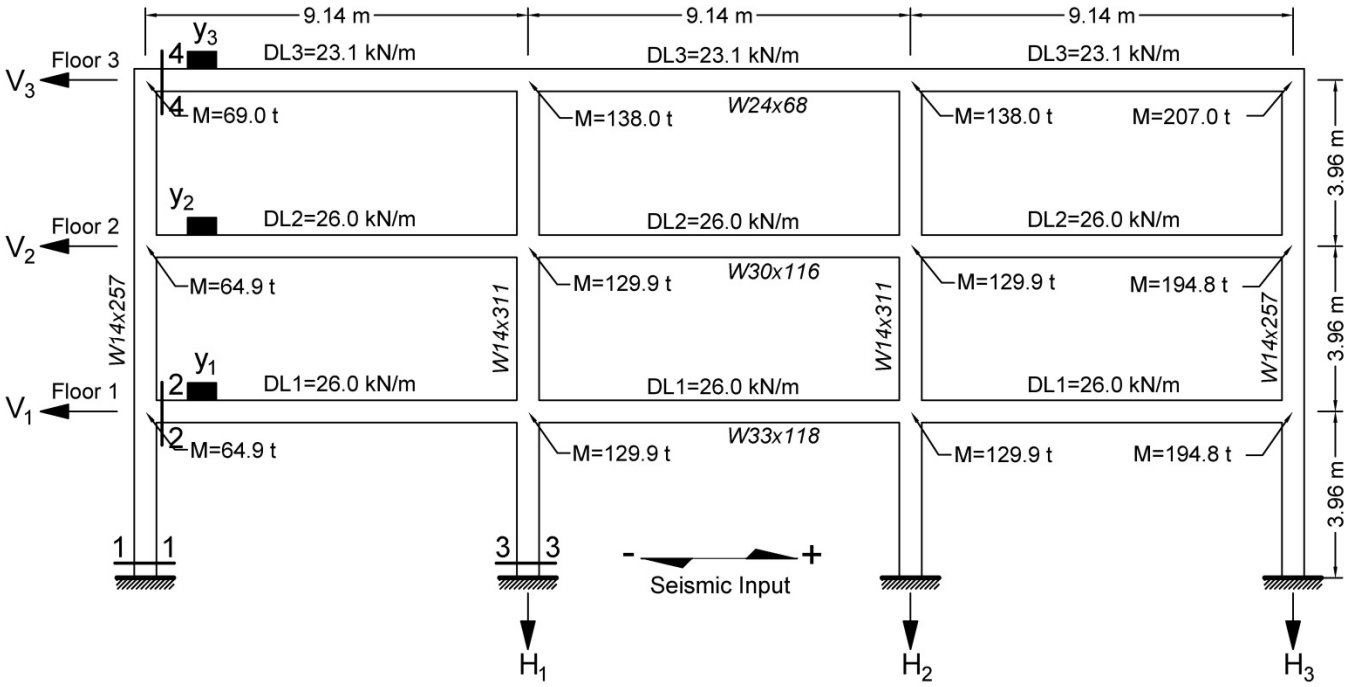

Figure 12. 3-story 3-bay steel frame model

Table 2. True material properties for columns and beams used for response simulation

	E (GPa)	f_y (MPa)	b
Columns	200	345	0.08
Beams	200	250	0.05

4.2 Modeling errors

The effects of modeling errors are included in this application by considering realistic inaccuracies in model geometry, mass properties, dead loads, damping properties, number of integration points (NIP) of beam-column elements, boundary conditions (BCs), and constitutive model for steel material as summarized in Table 3. Geometry errors are defined by varying the location of columns (H_1, H_2 and H_3) and beams (V_1, V_2 and V_3) relative to the bay-width (for H_i) or story-height (for V_i), e.g., an error coefficient of 1.03 for H_1 considers the new coordinate of column H_1 equals to H_1 + 0.03×bay-width. Only ±3% error is considered for geometry in this study since structural geometry can usually be measured with high accuracy. For errors in nodal masses, dead loads, and Rayleigh damping, the error

coefficients denote the scale factor of their true values, e.g., an error coefficient 0.8 for NM_1 indicates that all nodal masses on floor 1 are reduced 20% evenly. Note that nodal masses and dead loads on the same floor are modified evenly based on error coefficients. Parameters α_M and β_K refer to mass and stiffness proportional damping factors of Rayleigh damping, respectively. NIP for force-based beam-column element is an important parameter in nonlinear analysis and inappropriate NIP may introduce modeling errors in plastic hinge length. For boundary conditions errors, a combination of pins and rotational springs are considered instead of the perfectly fixed base, as shown in Figure 13(a). The rotational springs have a stiffness of 3×10^5 kN-m/rad . To account for modeling errors due to material constitutive model, a bilinear model is assumed to replace the original GMP model as shown in Figure 13(b).

A total of 21 updating models are created with different combinations of modeling errors as detailed in Table 4. The first 3 models have only geometric errors. Models 4 and 5 only have modeling errors in damping properties. Models 6 to 14 include combinations of errors in geometry, mass, dead load, damping, and NIP. Updating models 15 to 17 have pins and rotational springs as the boundary conditions, and models 18 to 21 use bilinear constitutive model for steel. The acceleration response comparisons between true model and updating Models 1–21 are shown in Figure 14. It can be seen that the modeling errors considered in the updating models have significant effects on the measured acceleration response which are much larger than the added noise level of 1% NSR. These modeling errors have the largest effects on the response of the first floor while have smaller effects on the third floor acceleration response.

Table 3. Modeling errors types and details

Modeling error types	Parameters	Modeling Error details
Geometry	H_1, H_2, H_3, V_1, V_2, V_3	±3% of bay-width (for H_i) or story-height (for V_i)
Nodal mass	NM_1, NM_2, NM_3	Nodal masses at the indexed story are scaled
Dead load	DL_1, DL_2, DL_3	Dead loads at the indexed story are scaled
Rayleigh damping	α_M, β_K	Mass and stiffness matrix factors are scaled
NIP for force-based beam-column element	NIP_c, NIP_b	Different NIPs are assigned for all column (NIP_c) and beam elements (NIP_b)
BCs	Fixed boundary or pin + rotational spring	Pin BCs with rotational springs are used at column bases instead of perfectly fixed
Constitutive model	GMP model or bilinear model	Bilinear steel model is used instead of GMP model

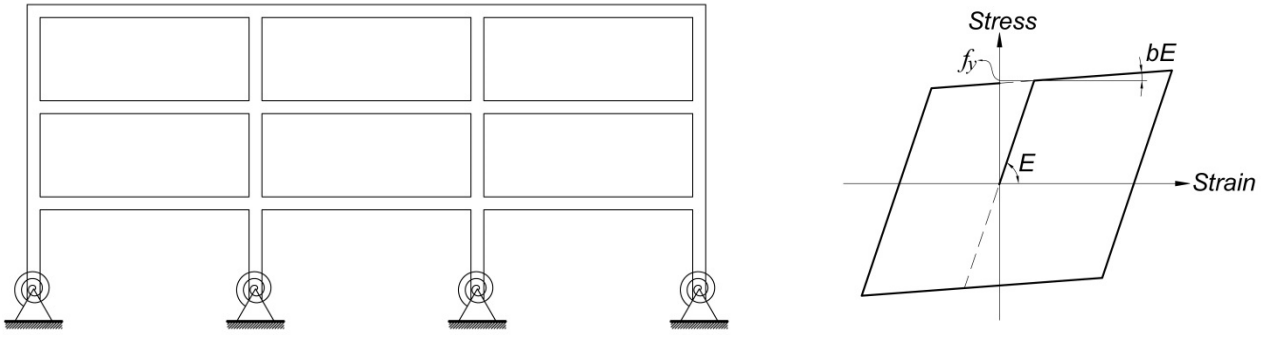

(a) (b)

Figure 13. (a) Modeling errors in boundary conditions, and (b) material model (bilinear model instead of GMP)

Table 4. Summary of modeling errors in the 21 updating models. Reported parameters are scaled to the true (or nominal) values, i.e., 1.0 refer to no modeling error except for NIP

Model ID	H_1	H_2	H_3	V_1	V_2	V_3	NM_1	NM_2	NM_3	DL_1	DL_2	DL_3	α_M	β_K	NIP_c	NIP_b
1	1.03	0.97	1.03	1.03	0.97	1.03	1	1	1	1	1	1	1	1	6	7
2	0.97	1.03	0.97	0.97	1.03	0.97	1	1	1	1	1	1	1	1	6	7
3	0.97	1.03	1.03	0.97	1.03	1.03	1	1	1	1	1	1	1	1	6	7
4	1	1	1	1	1	1	1	1	1	1	1	1	2	2	6	7
5	1	1	1	1	1	1	1	1	1	1	1	1	0.5	0.5	6	7
6	1.03	0.97	1.03	1.03	0.97	1.03	1.1	0.9	0.9	1.1	1.1	1.1	1	1	6	7
7	1.03	0.97	1.03	1.03	0.97	1.03	1.1	1	1	1.1	1.1	1.1	1.5	1.5	6	7
8	0.97	1.03	0.97	0.97	1	1	1	0.9	1.1	1.3	1.3	1.3	2	2	3	4
9	0.97	1	1	1.03	1	1	1	1.3	1	1	1.3	1	1.5	1.5	6	7
10	0.97	1.03	0.97	0.97	1.03	0.97	1	1.3	1	1.3	1.3	1.3	1	1	6	7
11	1.03	0.97	1.03	1.03	0.97	1.03	1.3	0.7	1.3	1.3	0.7	1.3	2	2	3	4
12	1.03	0.97	1.03	1.03	0.97	1.03	0.7	1	1.3	0.7	1	1.3	2	2	10	4
13	1.03	0.97	1.03	1.03	0.97	1.03	1.3	1	0.7	1.3	1	0.7	2	2	6	7
14	1.03	0.97	1	1.03	0.97	1	1.2	1	1.2	1.2	1	1.2	1.5	1.5	3	4
15_b	1	1	1	1	1	1	1	1	1	1	1	1	1	1	6	7
16_b	1.03	0.97	1.03	1.03	0.97	1.03	1	1.2	1	1	1.2	1	2	2	6	7
17_b	1.03	0.97	1.03	1.03	0.97	1.03	1	1	1.2	1.2	1.2	1.2	1.5	1.5	10	4
18_c	1	1	1	1	1	1	1	1	1	1	1	1	1	1	6	7
19_c	1	1	1	1	1	1	1.3	1	1	1.3	1.3	1.3	1.5	1.5	6	7
20_c	1	1	1	1	1	1	1	1.3	1	1.3	1.3	1.3	2	2	3	4
21_c	1.03	0.97	1.03	1.03	0.97	1.03	1	1	1	1	1	1	1.5	1.5	3	4

Note: subscript 'b' refers to modeling errors in BCs (pin BCs and rotational springs instead of perfectly fixed boundary); subscript 'c' refers to modeling errors in constitutive model for steel material (bilinear model instead of GMP model).

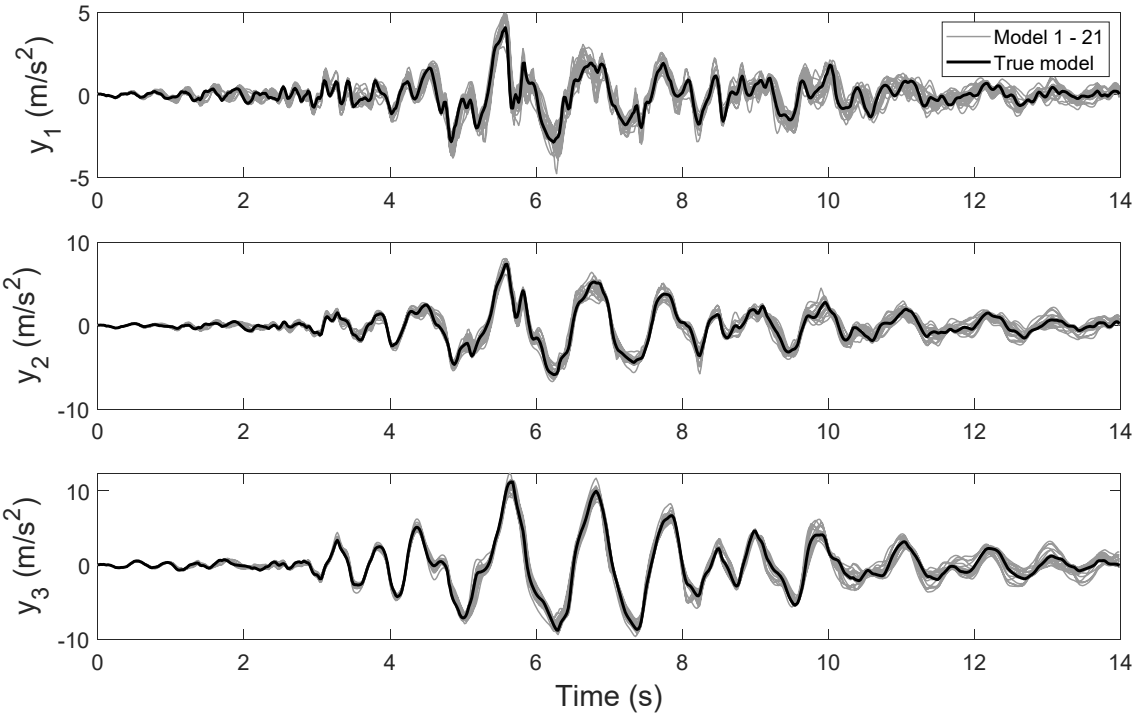

Figure 14. Acceleration response comparison for different updating models and true model using true parameter values

4.3 Model updating results

Model updating is performed using the non-adaptive and three adaptive UKF methods for all 21 updating models with different modeling errors. The updating parameters are selected as the material properties of columns and beams $\boldsymbol{\theta} = [E(\text{col})\ \ f_y(\text{col})\ \ b(\text{col})\ \ E(\text{beam})\ \ f_y(\text{beam})\ \ b(\text{beam})]^T$ which are normalized to their true values shown in Table 2. Initial values are $\hat{\boldsymbol{\theta}}_0^+ = \begin{bmatrix} 0.8 & 1.2 & 1.4 & 0.8 & 1.2 & 1.4 \end{bmatrix}^T$ with initial covariance matrix $\mathbf{P}_0^+ = diag\left(0.2\hat{\boldsymbol{\theta}}_0^+\right)^2$. The covariance of process noise is $\mathbf{Q} = diag\left(10^{-4}\hat{\boldsymbol{\theta}}_0^+\right)^2$. The true covariance matrix of added white noise $\mathbf{R}^{\text{noise}}$ is used for the non-adaptive UKF and as the initial value of $\mathbf{R}$ for adaptive UKFs. Note that due to the effects of modeling errors, the effective noise covariance matrix $\mathbf{R}$ is a time-variant variable and will be larger than $\mathbf{R}^{\text{noise}}$ to account for modeling errors. In the application of adaptive methods, factor α = 0.9 is selected for forgetting factor method, window size of 20 is chosen for moving window method, and $\mathbf{U} = 10^{-18} \times \mathbf{I}_3$ for dual adaptive method where $\mathbf{I}_3$ denotes identity matrix of size 3 by 3. These choices are selected to provide enough statistical smoothing of R estimation based on the previous observation in Application 1.

Model updating results using 21 updating models are shown in Figure 15. It can be seen that non-adaptive and adaptive methods provide similar results for Young's modulus E(col) and E(beam) due to their high sensitivities to measurement. Significant improvements are made by adaptive methods for f_y and b for both columns and beams, especially for b(col) and b(beam). Their estimation accuracies are improved, and estimation variabilities are reduced. This is due to the fact that f_y and b have lower sensitivity to the measurement, and therefore are most affected by the value of $\mathbf{R}$. These effects are mitigated by adopting adaptive UKFs through updating $\mathbf{R}$ recursively. The mean and standard deviation of parameter estimation errors over 21 cases are reported in Table 5. Parameter estimation error is defined as $\text{error} = \left|\theta_i^{\text{updated}} - \theta_i^{\text{true}}\right| / \theta_i^{\text{true}}$ in which $\theta_i^{\text{true}} = 1$, since the updating parameters are normalized to their true values. Similar observations can be made from Table 5, showing that significant error reductions have been achieved for f_y(col), b(col), f_y(beam) and b(beam) when using adaptive methods. Overall, the estimation errors across all parameters and cases (last two rows in Table 5) show a significant reduction of 66% in the mean values and 80% in the standard deviations. Generally, the three adaptive methods provide very similar estimation results, with forgetting factor method performing slightly better (smaller errors) in the present case study. The detailed parameter estimation results are reported in Appendix C.

The comparisons of parameter estimation and parameter uncertainty histories between non-adaptive and adaptive UKFs using Model 14 (Table 4) are shown in Figure 16 and Figure 17. It can be seen that parameters f_y(col), b(col), f_y(beam) and b(beam) converge to inaccurate values using the non-adaptive method. This can be justified by the fact that fixed $\mathbf{R}$ assigns uniform weight/trust on measurements along the response time history. Such uniform trust/weight should be avoided in the presence of substantial modeling errors and has been mitigated by using adaptive methods through updating $\mathbf{R}$ recursively. Young's modulus of columns E(col) is overestimated by both the non-adaptive and adaptive methods in order to compensate the over-assigned mass property in Model 14. Parameter uncertainty using non-adaptive method is drastically underestimated (Figure 17) due to the use of fixed $\mathbf{R}$. This uncertainty is not accurate and is unrealistic for uncertainty quantification or response prediction. Larger and more realistic parameter uncertainty is obtained by adaptive methods.

The comparisons of acceleration response predictions are shown in Figure 18 when using Model 14. The response predictions are obtained from the corresponding updated model and the Loma Prieta earthquake input motion. It can be seen that considerable discrepancies exist between predictions and measurement for non-adaptive method due to the poor estimated parameter values. However, acceleration predictions using adaptive methods match the measurements well. To further investigate the prediction capabilities of the updated model in presence of modeling errors, un-measured response predictions including base shear (V) vs. roof drift ratio and section moment vs. curvature at sections 1-1 and 2-2 (M_{1-1} vs. κ_{1-1}, M_{2-2} vs. κ_{2-2}), flange stress-strain response at sections 3-3 and 4-4 (σ_{3-3} vs. ε_{3-3} and σ_{4-4} vs. ε_{4-4}), are shown in Figure 19 (refer to Figure 12 for the specified locations). It can be seen that local response predictions are substantially improved by adaptive methods. The predictions from adaptive methods for base shear vs. roof drift ratio, M_{2-2} vs. κ_{2-2}, and σ_{4-4} vs. ε_{4-4} agree with their true counterparts. These local responses are important quantities for structural health assessment and their prediction accuracy is critical for damage identification. Statistics of the relative root-mean-square errors (RRMSE) of response predictions for all 21 updating models are shown in Figure 20 as box plots and reported in Table 6. The RRMSE for a response signal **a** is defined as:

$$\text{RRMSE}(\mathbf{a}) = \frac{\text{RMS}(\mathbf{a}-\mathbf{a}^{\text{true}})}{\text{RMS}(\mathbf{a}^{\text{true}})}\times 100\% \tag{10}$$

It can be observed that adaptive methods significantly reduce the RRMSE for all of the response predictions by an average of almost 50%.

The modeling errors considered in this study add significant bias to structural response as observed in Figure 14. Figure 21 provides a comparison between estimated noise covariance and the nominal values at three measurement channels for Model 14. The nominal covariance is defined as $\mathbf{R}_k^{\text{nominal}} = diag\left(\left[\mathbf{y}^{\text{true}}(k)-\mathbf{y}^{\text{error}}(k)\right]\left[\mathbf{y}^{\text{true}}(k)-\mathbf{y}^{\text{error}}(k)\right]^T\right)+\mathbf{R}_k^{\text{noise}}$, where $\mathbf{y}^{\text{true}}$ and $\mathbf{y}^{\text{error}}$ represent the acceleration response of the true model and updating model (with modeling errors) using the true parameter values, and $\mathbf{R}_k^{\text{noise}}$ is the covariance of polluted noise of 1% NSR. From Figure 21, it can be seen that the nominal covariance fluctuates drastically while the estimated values change smoothly following the trend of nominal covariance. The estimated covariance values can be significantly smaller than the nominal values at certain time steps. It is worth noting that there is no true noise covariance available in this case and the nominal value as defined above, compensates the effects of response bias caused by modeling errors. However, the parameter estimation results have been improved significantly by updating the noise covariance adaptively to account for the effects of modeling errors.

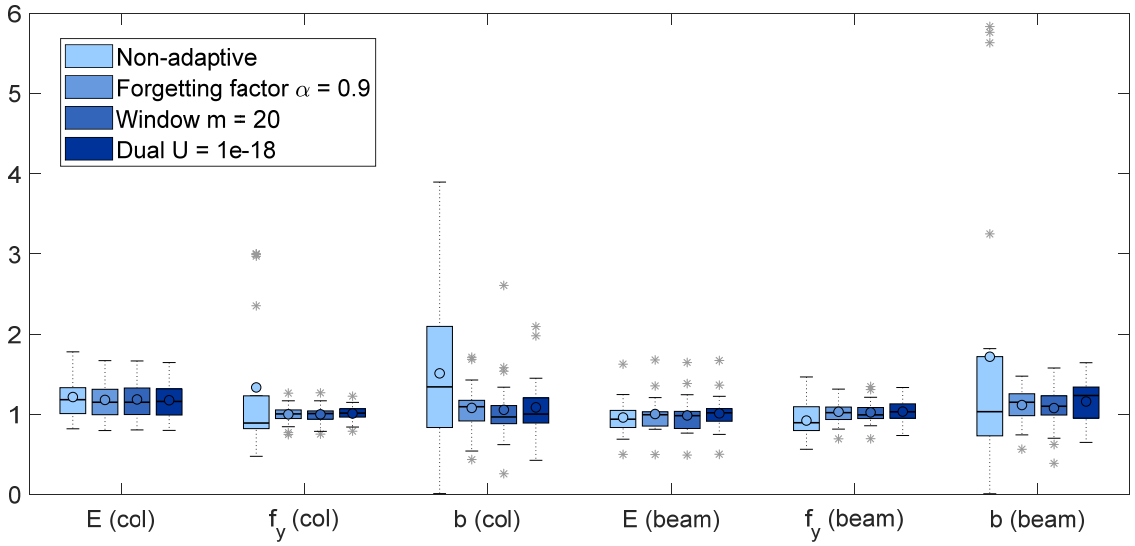

Figure 15. Boxplot of model updating results using 21 updating models (circles refer to mean values and stars are outliers)

Table 5. Summary of parameter estimation errors

	Non-adaptive	Forgetting factor	Window	Dual
E (col)	0.25 / 0.23	0.23 / 0.19	0.24 / 0.19	0.23 / 0.19
f_y (col)	0.60 / 0.74	0.09 / 0.08	0.09 / 0.08	0.07 / 0.07
b (col)	0.91 / 0.77	0.24 / 0.21	0.28 / 0.36	0.29 / 0.31
E (beam)	0.16 / 0.16	0.15 / 0.17	0.17 / 0.17	0.15 / 0.17
f_y (beam)	0.21 / 0.15	0.11 / 0.10	0.10 / 0.10	0.12 / 0.10
b (beam)	1.12 / 1.59	0.22 / 0.13	0.22 / 0.18	0.26 / 0.16
Mean	0.54	0.17	0.18	0.19
Std	0.86	0.16	0.21	0.19

Note: Cell value format is mean/standard deviation (std) over all cases; Last two rows represent mean and std over all cases and parameters.

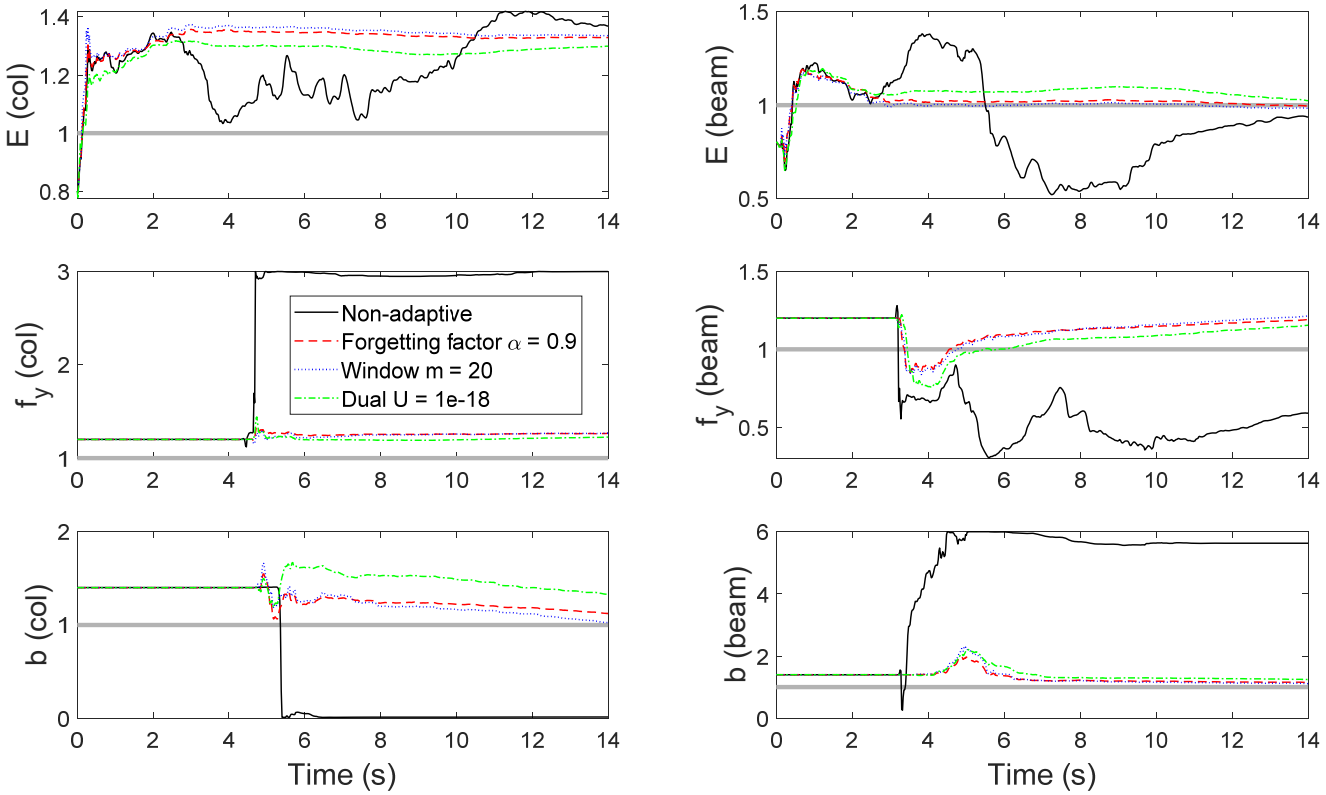

Figure 16. Parameter estimation histories using non-adaptive and adaptive KFs for Model 14

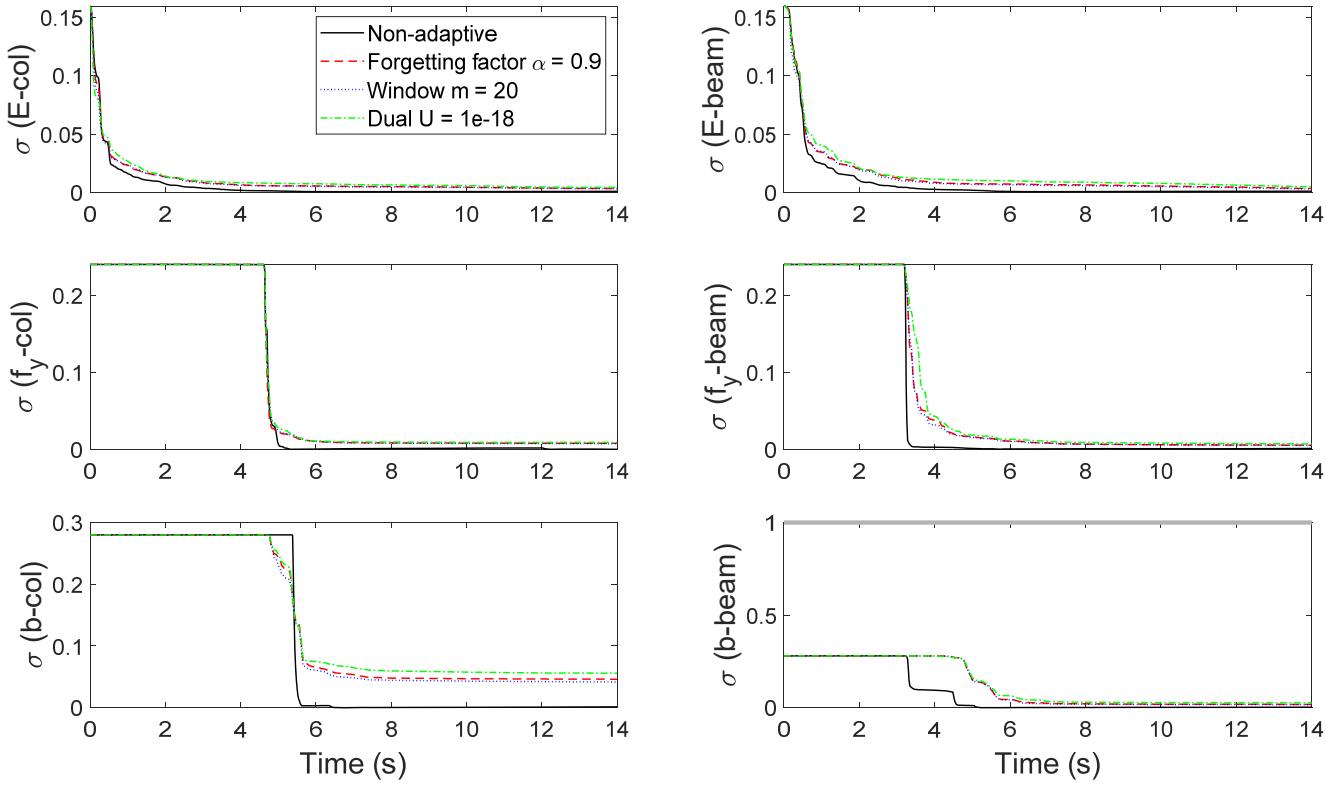

Figure 17. Parameter uncertainty estimation histories using non-adaptive and adaptive KFs for Model 14

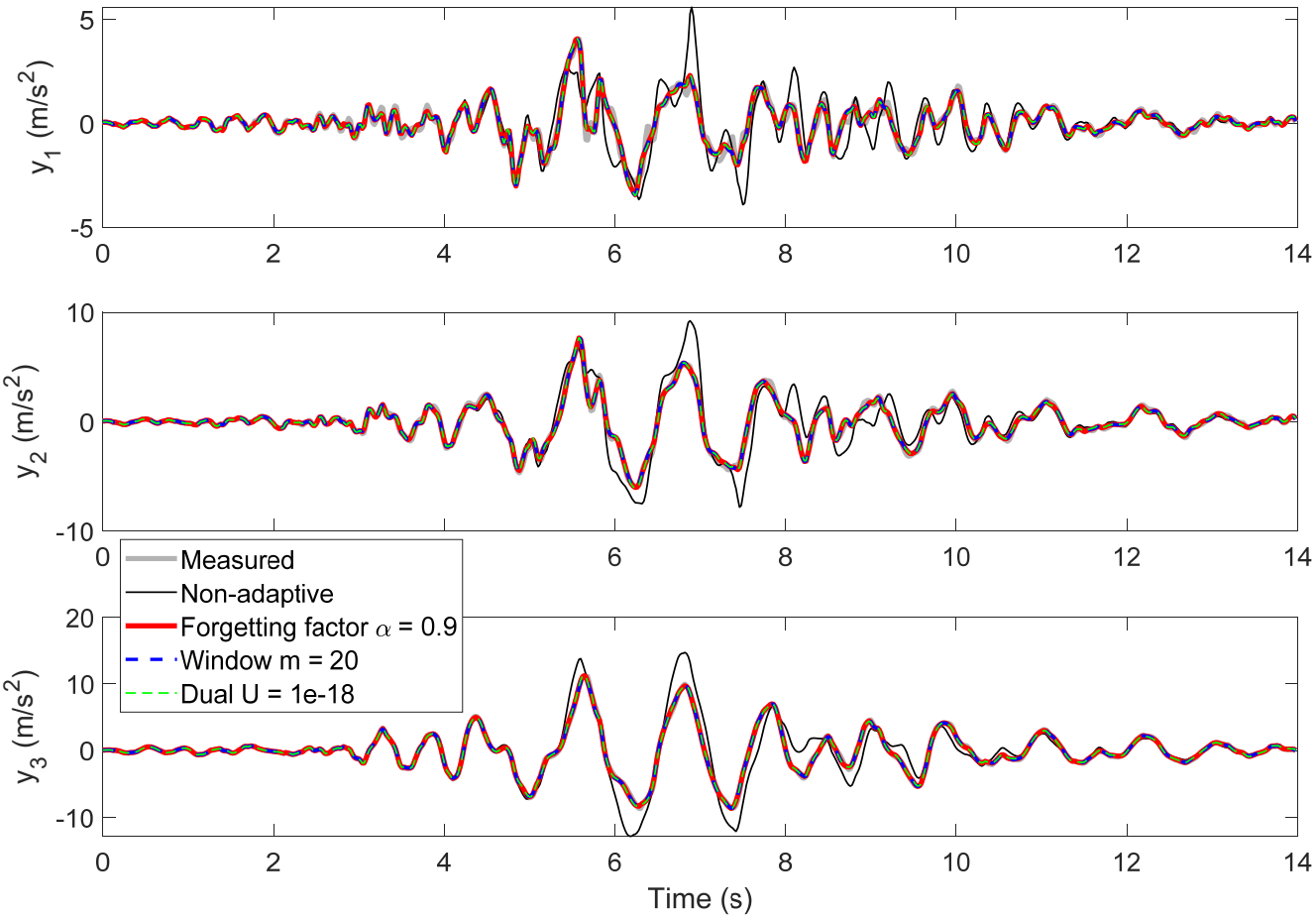

Figure 18. Comparison of predicted acceleration response using non-adaptive and adaptive KFs for Model 14

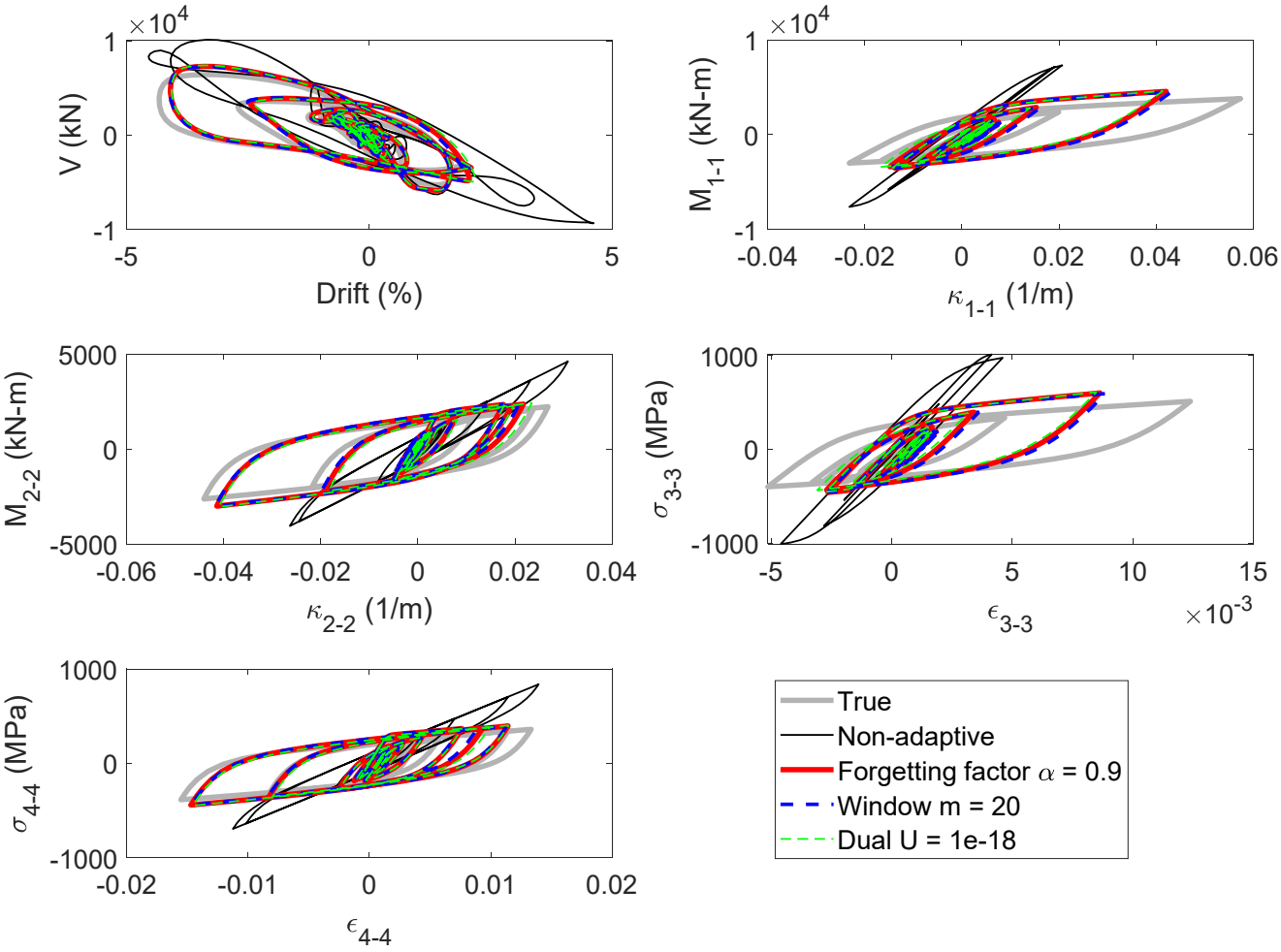

Figure 19. Comparison of un-measured response predictions using non-adaptive and adaptive KFs for Model 14

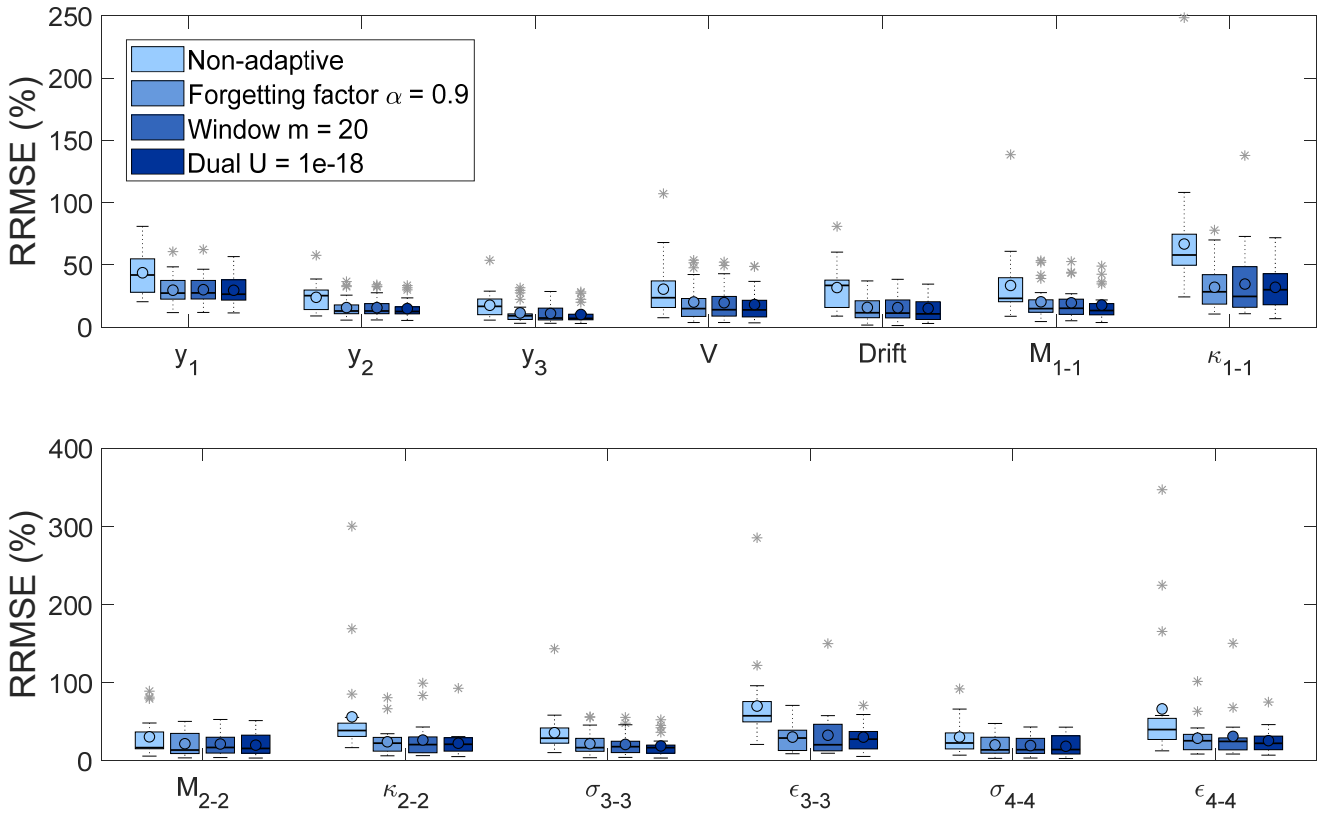

Figure 20. RRMSE of response predictions using non-adaptive and adaptive KFs over 21 updating models

Table 6. RRMSE (%) of measured and un-measured response predictions

	Non-adaptive	Forgetting factor	Window	Dual
y_1	44 / 17	30 / 12	30 / 12	30 / 12
y_2	24 / 12	16 / 9	16 / 9	15 / 8
y_3	18 / 11	11 / 9	11 / 8	10 / 8
V	30 / 24	20 / 16	20 / 14	18 / 14
Drift	32 / 19	16 / 11	16 / 12	15 / 11
M_{1-1}	33 / 28	20 / 14	20 / 13	18 / 13
κ_{1-1}	67 / 46	32 / 19	35 / 29	32 / 19
M_{2-2}	31 / 25	22 / 16	21 / 14	20 / 14
κ_{2-2}	56 / 65	24 / 19	26 / 24	22 / 19
σ_{3-3}	36 / 28	22 / 16	21 / 14	19 / 14
ϵ_{3-3}	70 / 55	30 / 18	33 / 32	30 / 18
σ_{4-4}	30 / 21	20 / 14	19 / 13	19 / 13
ϵ_{4-4}	66 / 82	29 / 21	31 / 31	26 / 16
Mean	41	23	23	21
Std	33	15	17	14

Note: Cell value format is mean/standard deviation (std) over all cases; Last two rows represent mean and std over all cases and parameters.

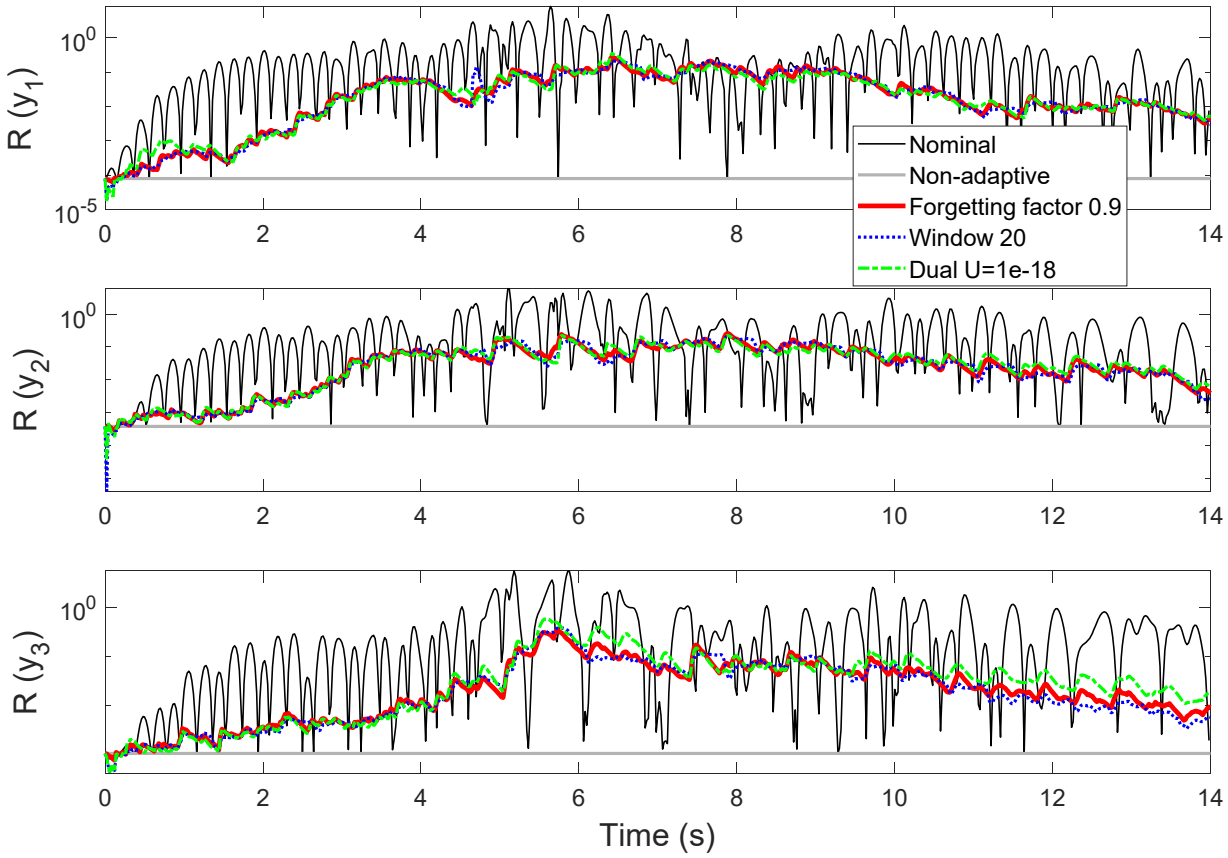

Figure 21. Comparison of estimated noise covariance with nominal values for Model 14

5. Summary and Conclusions

Two adaptive KF methods, namely the forgetting factor method and the moving window method, which were previously used in electrical engineering applications, are employed in this study for model updating of nonlinear dynamic systems where the covariance of measurement noise is estimated recursively. The adaptive methods are formulated using covariance-matching technique based on either innovation or residual. In this study the residual-based approaches are implemented to two numerical applications and compared with non-adaptive UKF and an existing dual adaptive UKF method. The proposed adaptive algorithm can be integrated with any nonlinear KF for state estimation, parameter estimation or joint state-parameter estimation, e.g., EKF, UKF and EnKF. Performance of the non-adaptive and adaptive KFs are first evaluated for model updating of a cantilever steel pier with no consideration of modeling errors. It is found that the non-adaptive UKF provides poor estimation for selected updating parameters when the noise covariance is unknown and a wrong **R** is used. In contrast, accurate results are achieved by all three adaptive filters (forgetting factor, moving window and dual adaptive). The performance of the proposed adaptive filters is further investigated when applied to 3-story 3-bay steel moment resisting frame with substantial modeling errors. A total of 21 updating models are created with modeling errors in geometry, mass properties, dead loads, damping properties, NIP for force-based beam-column element, BCs and constitutive model for steel material. Based on the numerical applications, the following observations are made.

(1) Although formulated differently using different covariance-matching techniques, the three adaptive methods (forgetting factor, moving window and dual adaptive) generally provide similar performance.
(2) In the considered case studies, the results did not show sensitivity to the values of α and m, parameters of the forgetting factor and moving windows methods, respectively. In general, values of α in the range of 0.7 to 0.9, and value of m in the range of 10 to 30 are recommended for structural systems with similar dynamic properties as the ones considered here.
(3) Larger values in factor α (forgetting factor method), window size m (moving window method) and parameter **U** (dual adaptive method) would provide more statistical smoothing in **R** estimation.
(4) Residual-based adaptive methods (forgetting factor and moving window) are capable of estimating the full matrix of **R** (with off-diagonal entries containing information about noise/modeling errors correlation) and ensuring its positive definiteness. On the contrary, only diagonal terms of **R** can be estimated and a lower bound has to be assigned to assure its positive definiteness using innovation-based dual adaptive filter.
(5) Compared to non-adaptive KF, the proposed adaptive methods generally improve the accuracy of parameter estimation and uncertainty quantification when wrong **R** is used (Application 1) or at the existence of substantial modeling errors (Application 2). In addition, the adaptive filters can estimate the true **R** with acceptable accuracy.

Acknowledgements

The authors acknowledge partial support of this study by the National Science Foundation Grants 1254338 and 1903972. Rodrigo Astroza acknowledges the financial support from the Chilean National Commission for Scientific and Technological Research (CONICYT), FONDECYT project No. 11160009. The opinions, findings, and conclusions expressed in this paper are those of the authors and do not necessarily represent the views of the sponsors and organizations involved in this project.

Appendix A: Derivation of innovation-based covariance matching function

The derivation of innovation-based covariance-matching function is provided in this section. The state space model for a linear KF is shown below:

$$\begin{cases} \mathbf{x}_k = \mathbf{A}_{k-1}\mathbf{x}_{k-1} + \mathbf{B}_{k-1}\mathbf{u}_{k-1} + \mathbf{w}_{k-1} \\ \mathbf{y}_k = \mathbf{H}_k\mathbf{x}_k + \mathbf{D}_k\mathbf{u}_k + \mathbf{v}_k \end{cases} \tag{A1}$$

Two types of estimation errors (prior error $\mathbf{e}_k^-$ and posterior error $\mathbf{e}_k^+$) are defined below:

$$\mathbf{e}_k^- = \mathbf{x}_k - \hat{\mathbf{x}}_k^- \tag{A2}$$

$$\mathbf{e}_k^+ = \mathbf{x}_k - \hat{\mathbf{x}}_k^+ \tag{A3}$$

The innovation can be derived as

$$\mathbf{d}_k = \mathbf{y}_k - (\mathbf{H}_k\hat{\mathbf{x}}_k^- + \mathbf{D}_k\mathbf{u}_k) = \mathbf{H}_k\mathbf{x}_k + \mathbf{D}_k\mathbf{u}_k + \mathbf{v}_k - (\mathbf{H}_k\hat{\mathbf{x}}_k^- + \mathbf{D}_k\mathbf{u}_k) = \mathbf{H}_k(\mathbf{x}_k - \hat{\mathbf{x}}_k^-) + \mathbf{v}_k = \mathbf{H}_k\mathbf{e}_k^- + \mathbf{v}_k \tag{A4}$$

The covariance of innovation is derived as

$$
\begin{aligned}
E\left[\mathbf{d}_k\mathbf{d}_k^T\right] &= E\left[\left(\mathbf{H}_k\mathbf{e}_k^- + \mathbf{v}_k\right)\left(\mathbf{H}_k\mathbf{e}_k^- + \mathbf{v}_k\right)^T\right] \\
&= E\left[\mathbf{H}_k\mathbf{e}_k^-\mathbf{e}_k^{-T}\mathbf{H}_k^T + \mathbf{H}_k\mathbf{e}_k^-\mathbf{v}_k^T + \mathbf{v}_k\mathbf{e}_k^{-T}\mathbf{H}_k^T + \mathbf{v}_k\mathbf{v}_k^T\right] \\
&= \mathbf{H}_k E\left[\mathbf{e}_k^-\mathbf{e}_k^{-T}\right]\mathbf{H}_k^T + E\left[\mathbf{v}_k\mathbf{v}_k^T\right] \\
&= \mathbf{H}_k\mathbf{P}_k^-\mathbf{H}_k^T + \mathbf{R}_k
\end{aligned}
\tag{A5}
$$

This is based on the fact that $\mathbf{e}_k^-$ and $\mathbf{v}_k$ are uncorrelated, i.e., $E\left[\mathbf{e}_k^-\mathbf{v}_k^T\right] = E\left[\mathbf{v}_k\mathbf{e}_k^{-T}\right] = \mathbf{0}$. Therefore, the innovation-based covariance-matching function is obtained:

$$
\mathbf{R}_k = E\left[\mathbf{d}_k\mathbf{d}_k^T\right] - \mathbf{H}_k\mathbf{P}_k^-\mathbf{H}_k^T \tag{A6}
$$

Appendix B: Derivation of residual-based covariance matching function

The derivation of residual-based covariance-matching function is provided in this section. The residual can be expressed in terms of the posterior error $\mathbf{e}_k^+$ as

$$
\boldsymbol{\varepsilon}_k = \mathbf{y}_k - (\mathbf{H}_k\hat{\mathbf{x}}_k^+ + \mathbf{D}_k\mathbf{u}_k) = \mathbf{H}_k\mathbf{x}_k + \mathbf{D}_k\mathbf{u}_k + \mathbf{v}_k - (\mathbf{H}_k\hat{\mathbf{x}}_k^+ + \mathbf{D}_k\mathbf{u}_k) = \mathbf{H}_k(\mathbf{x}_k - \hat{\mathbf{x}}_k^+) + \mathbf{v}_k = \mathbf{H}_k\mathbf{e}_k^+ + \mathbf{v}_k \tag{B1}
$$

The covariance of residual can be formulated below:

$$
\begin{aligned}
E\left[\boldsymbol{\varepsilon}_k\boldsymbol{\varepsilon}_k^T\right] &= E\left[\left(\mathbf{H}_k\mathbf{e}_k^+ + \mathbf{v}_k\right)\left(\mathbf{H}_k\mathbf{e}_k^+ + \mathbf{v}_k\right)^T\right] \\
&= E\left[\mathbf{H}_k\mathbf{e}_k^+\mathbf{e}_k^{+T}\mathbf{H}_k^T + \mathbf{H}_k\mathbf{e}_k^+\mathbf{v}_k^T + \mathbf{v}_k\mathbf{e}_k^{+T}\mathbf{H}_k^T + \mathbf{v}_k\mathbf{v}_k^T\right] \\
&= \mathbf{H}_k\mathbf{P}_k^+\mathbf{H}_k^T + E\left[\mathbf{H}_k\mathbf{e}_k^+\mathbf{v}_k^T\right] + E\left[\mathbf{v}_k\mathbf{e}_k^{+T}\mathbf{H}_k^T\right] + \mathbf{R}_k
\end{aligned}
\tag{B2}
$$

The term $E\left[\mathbf{H}_k\mathbf{e}_k^+\mathbf{v}_k^T\right]$ in Eq. (B2) can be expanded as

$$
\begin{aligned}
E\left[\mathbf{H}_k\mathbf{e}_k^+\mathbf{v}_k^T\right] &= \mathbf{H}_k E\left[\left(\mathbf{x}_k - \hat{\mathbf{x}}_k^+\right)\mathbf{v}_k^T\right] \\
&= \mathbf{H}_k E\left[\mathbf{x}_k\mathbf{v}_k^T - \hat{\mathbf{x}}_k^+\mathbf{v}_k^T\right] \\
&= -\mathbf{H}_k E\left[\hat{\mathbf{x}}_k^+\mathbf{v}_k^T\right] \\
&= -\mathbf{H}_k E\left[\left(\hat{\mathbf{x}}_k^- + \mathbf{K}_k\left(\mathbf{y}_k - \mathbf{H}_k\hat{\mathbf{x}}_k^- - \mathbf{D}_k\mathbf{u}_k\right)\right)\mathbf{v}_k^T\right] \\
&= -\mathbf{H}_k E\left[\left(\hat{\mathbf{x}}_k^- + \mathbf{K}_k\left(\mathbf{H}_k\mathbf{e}_k^- + \mathbf{v}_k\right)\right)\mathbf{v}_k^T\right] \\
&= -\mathbf{H}_k E\left[\hat{\mathbf{x}}_k^-\mathbf{v}_k^T + \mathbf{K}_k\mathbf{H}_k\mathbf{e}_k^-\mathbf{v}_k^T + \mathbf{K}_k\mathbf{v}_k\mathbf{v}_k^T\right] \\
&= -\mathbf{H}_k\mathbf{K}_k\mathbf{R}_k
\end{aligned}
\tag{B3}
$$

in which the following facts are applied: $\mathbf{x}_k$, prior estimate $\hat{\mathbf{x}}_k^-$, and prior error $\mathbf{e}_k^-$ are all uncorrelated with $\mathbf{v}_k$.

The term $E\left[\mathbf{v}_k\mathbf{e}_k^{+T}\mathbf{H}_k^T\right]$ in Eq. (B2) is derived below by using result from Eq. (B3):

$$E\left[\mathbf{v}_k\mathbf{e}_k^{+T}\mathbf{H}_k^T\right]=E\left[\left(\mathbf{H}_k\mathbf{e}_k^+\mathbf{v}_k^T\right)^T\right]=E\left[\mathbf{H}_k\mathbf{e}_k^+\mathbf{v}_k^T\right]^T=\left(-\mathbf{H}_k\mathbf{K}_k\mathbf{R}_k\right)^T=-\mathbf{R}_k\mathbf{K}_k^T\mathbf{H}_k^T \tag{B4}$$

Therefore, the covariance of residual is formulated below by substituting results from Eq. (B3) and Eq. (B4):

$$E\left[\boldsymbol{\varepsilon}_k\boldsymbol{\varepsilon}_k^T\right]=\mathbf{H}_k\mathbf{P}_k^+\mathbf{H}_k^T-\mathbf{H}_k\mathbf{K}_k\mathbf{R}_k-\mathbf{R}_k\mathbf{K}_k^T\mathbf{H}_k^T+\mathbf{R}_k \tag{B5}$$

It can be proved that $\mathbf{H}_k\mathbf{P}_k^+\mathbf{H}_k^T$ and $\mathbf{H}_k\mathbf{K}_k\mathbf{R}_k$ are equal as shown below:

$$\begin{aligned}\mathbf{H}_k\mathbf{P}_k^+\mathbf{H}_k^T-\mathbf{H}_k\mathbf{K}_k\mathbf{R}_k&=\mathbf{H}_k\left(\mathbf{I}-\mathbf{K}_k\mathbf{H}_k\right)\mathbf{P}_k^-\mathbf{H}_k^T-\mathbf{H}_k\mathbf{K}_k\mathbf{R}_k\\&=\mathbf{H}_k\mathbf{P}_k^-\mathbf{H}_k^T-\mathbf{H}_k\mathbf{K}_k\mathbf{H}_k\mathbf{P}_k^-\mathbf{H}_k^T-\mathbf{H}_k\mathbf{K}_k\mathbf{R}_k\\&=\mathbf{H}_k\mathbf{P}_k^-\mathbf{H}_k^T-\mathbf{H}_k\mathbf{K}_k\left(\mathbf{H}_k\mathbf{P}_k^-\mathbf{H}_k^T+\mathbf{R}_k\right)\\&=\mathbf{H}_k\mathbf{P}_k^-\mathbf{H}_k^T-\mathbf{H}_k\mathbf{P}_k^-\mathbf{H}_k^T\left(\mathbf{H}_k\mathbf{P}_k^-\mathbf{H}_k^T+\mathbf{R}_k\right)^{-1}\left(\mathbf{H}_k\mathbf{P}_k^-\mathbf{H}_k^T+\mathbf{R}_k\right)\\&=\mathbf{H}_k\mathbf{P}_k^-\mathbf{H}_k^T-\mathbf{H}_k\mathbf{P}_k^-\mathbf{H}_k^T\\&=\mathbf{0}\end{aligned} \tag{B6}$$

in which $\mathbf{P}_k^+=\left(\mathbf{I}-\mathbf{K}_k\mathbf{H}_k\right)\mathbf{P}_k^-$ and Kalman gain $\mathbf{K}_k=\mathbf{P}_k^-\mathbf{H}_k^T\left(\mathbf{H}_k\mathbf{P}_k^-\mathbf{H}_k^T+\mathbf{R}_k\right)^{-1}$ have been substituted. Therefore, it is easy to show that $\mathbf{R}_k\mathbf{K}_k^T\mathbf{H}_k^T$ is also equal to $\mathbf{H}_k\mathbf{P}_k^+\mathbf{H}_k^T$:

$$\mathbf{R}_k\mathbf{K}_k^T\mathbf{H}_k^T=\left(\mathbf{H}_k\mathbf{K}_k\mathbf{R}_k\right)^T=\left(\mathbf{H}_k\mathbf{P}_k^+\mathbf{H}_k^T\right)^T=\mathbf{H}_k\mathbf{P}_k^+\mathbf{H}_k^T \tag{B7}$$

Finally, the residual-based covariance-matching function is obtained from Eq. (B5) by applying the results of Eq. (B6) and Eq. (B7):

$$E\left[\boldsymbol{\varepsilon}_k\boldsymbol{\varepsilon}_k^T\right]=\mathbf{R}_k-\mathbf{H}_k\mathbf{P}_k^+\mathbf{H}_k^T \tag{B8}$$

Appendix C: Summary of model updating results

Case		E (col)	f_y (col)	b (col)	E (beam)	f_y (beam)	b (beam)
1	Non-adaptive	1.21	2.97	1.28	0.94	0.95	1.22
	Forgetting factor	1.22	1.00	0.92	0.95	0.92	1.37
	Window	1.24	1.01	0.86	0.92	0.96	1.23
	Dual	1.22	0.99	0.95	0.93	0.92	1.33
2	Non-adaptive	0.93	0.82	0.31	1.04	0.92	0.73
	Forgetting factor	0.83	0.96	1.40	1.00	1.00	0.95
	Window	0.83	0.94	1.54	1.01	0.99	0.97
	Dual	0.84	1.02	0.77	1.04	1.05	0.85
3	Non-adaptive	0.98	0.90	0.41	1.06	1.03	0.80
	Forgetting factor	0.92	0.99	0.88	1.11	1.03	0.98
	Window	0.92	0.98	0.88	1.11	1.03	0.99
	Dual	0.95	0.99	0.88	1.07	1.03	0.95
4	Non-adaptive	1.01	2.99	1.42	0.94	1.10	1.32
	Forgetting factor	1.01	0.93	1.09	0.94	0.93	1.48
	Window	1.01	0.92	1.02	0.93	0.94	1.46
	Dual	1.01	0.96	1.00	0.94	0.97	1.39
5	Non-adaptive	1.00	0.89	0.83	1.05	0.95	0.78
	Forgetting factor	1.00	1.03	0.93	1.03	1.00	0.83
	Window	1.00	1.03	0.92	1.03	0.99	0.81

	Dual	0.99	1.02	1.00	1.04	1.01	0.85
6	Non-adaptive	1.27	0.87	2.09	0.76	0.88	1.16
	Forgetting factor	1.25	0.99	0.93	0.85	0.82	1.26
	Window	1.31	1.01	0.88	0.76	0.86	1.10
	Dual	1.32	1.02	0.89	0.75	0.87	0.95
7	Non-adaptive	1.33	3.00	1.14	0.84	1.09	0.93
	Forgetting factor	1.39	1.06	0.89	0.81	0.95	1.29
	Window	1.39	1.04	0.88	0.80	0.95	1.37
	Dual	1.36	1.05	0.99	0.83	0.95	1.25
8	Non-adaptive	0.91	1.04	1.32	1.04	1.31	0.75
	Forgetting factor	0.93	1.00	0.97	1.03	1.12	1.15
	Window	0.92	1.01	1.07	1.04	1.11	1.21
	Dual	0.90	1.01	1.07	1.07	1.13	1.21
9	Non-adaptive	1.20	1.16	1.56	0.95	1.14	0.51
	Forgetting factor	1.15	1.09	1.32	1.01	1.06	1.11
	Window	1.15	1.08	1.34	1.01	1.07	1.10
	Dual	1.16	1.09	1.45	1.00	1.03	1.13
10	Non-adaptive	1.08	0.75	2.23	0.97	0.84	0.01
	Forgetting factor	1.09	1.05	1.71	0.82	1.06	0.56
	Window	1.09	1.08	1.12	0.82	1.08	0.39
	Dual	0.97	1.07	1.34	1.02	1.11	0.71
11	Non-adaptive	1.52	0.57	3.13	0.92	1.46	0.63
	Forgetting factor	1.26	1.17	1.11	1.03	1.27	1.18
	Window	1.32	1.17	0.94	0.83	1.09	0.62
	Dual	1.27	1.15	1.13	1.05	1.26	1.33
12	Non-adaptive	0.82	0.83	3.89	1.62	1.24	1.82
	Forgetting factor	0.80	0.94	0.54	1.68	1.31	1.20
	Window	0.81	0.98	0.26	1.65	1.35	1.24
	Dual	0.80	0.97	0.54	1.67	1.33	1.23
13	Non-adaptive	1.59	2.35	0.01	0.50	0.85	0.28
	Forgetting factor	1.67	1.10	1.17	0.50	0.69	0.74
	Window	1.67	1.16	0.78	0.49	0.70	0.70
	Dual	1.65	1.09	0.97	0.50	0.74	0.65
14	Non-adaptive	1.37	3.00	0.01	0.94	0.59	5.63
	Forgetting factor	1.33	1.26	1.12	1.00	1.19	1.15
	Window	1.34	1.27	1.03	0.98	1.21	1.11
	Dual	1.30	1.23	1.33	1.02	1.15	1.24
15	Non-adaptive	1.18	0.68	1.35	1.25	0.90	1.50
	Forgetting factor	1.15	0.77	1.12	1.21	0.93	1.21
	Window	1.13	0.79	0.97	1.24	1.00	1.11
	Dual	1.15	0.79	1.15	1.22	1.01	0.98
16	Non-adaptive	1.75	0.85	1.34	1.05	0.80	5.83
	Forgetting factor	1.61	0.75	0.80	1.13	1.05	1.38
	Window	1.62	0.75	0.70	1.13	1.08	1.31
	Dual	1.63	0.84	0.43	1.12	1.14	1.34
17	Non-adaptive	1.78	0.48	1.89	1.19	0.85	5.76
	Forgetting factor	1.47	0.85	0.44	1.35	1.31	1.05
	Window	1.45	0.83	0.62	1.38	1.31	1.09
	Dual	1.45	0.88	0.48	1.36	1.33	1.03
18	Non-adaptive	1.04	0.71	1.12	0.80	0.58	1.03
	Forgetting factor	0.99	0.95	1.08	0.99	0.96	1.36
	Window	0.98	0.92	1.11	0.99	0.99	1.08
	Dual	1.00	0.95	1.20	0.99	0.96	1.37
19	Non-adaptive	1.30	1.23	0.25	0.69	0.60	0.39
	Forgetting factor	1.31	1.02	1.12	0.84	0.93	1.10
	Window	1.33	0.99	1.09	0.82	0.94	0.99
	Dual	1.32	1.02	1.16	0.83	0.89	1.46

20	Non-adaptive	1.11	1.08	2.87	0.84	0.70	1.72
	Forgetting factor	1.10	1.08	1.68	0.96	1.09	1.25
	Window	1.08	1.02	2.61	0.95	0.93	1.58
	Dual	1.15	1.09	1.98	0.91	1.04	1.44
21	Non-adaptive	1.15	0.86	3.24	0.78	0.56	3.25
	Forgetting factor	1.31	1.05	1.43	0.83	1.02	0.81
	Window	1.32	1.02	1.58	0.80	0.95	1.16
	Dual	1.24	1.00	2.09	0.87	0.80	1.64

Appendix D: Effects of different categories of modeling errors on the structural response

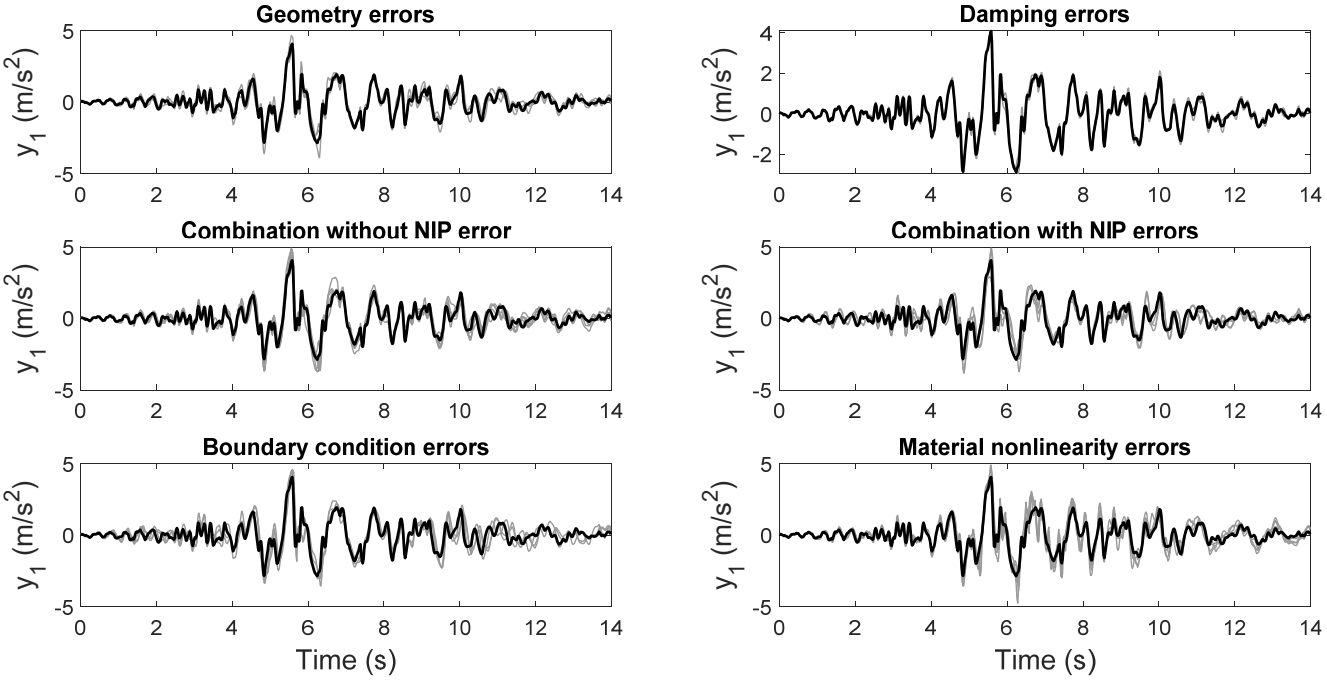

Figure D1. First floor acceleration response comparison between updating models (grey lines) and true model (black line) for different categories of modeling errors. Models 1-3 for geometric errors, Models 4-5 for errors in damping, Models 6-7, 9-10 and 13 for error combinations except NIP, Models 8, 11-12 and 14 for error combination including NIP errors, Models 15-17 for boundary condition errors, and Models 18-21 for material nonlinearity errors.

Reference

1. Brownjohn JM and Xia P-Q. Dynamic assessment of curved cable-stayed bridge by model updating. *Journal of structural engineering* 2000; 126: 252-260.
2. Brownjohn JMW, Moyo P, Omenzetter P and Lu Y. Assessment of highway bridge upgrading by dynamic testing and finite-element model updating. *Journal of Bridge Engineering* 2003; 8: 162-172.
3. Zhang Q, Chang T-YP and Chang CC. Finite-element model updating for the Kap Shui Mun cable-stayed bridge. *Journal of Bridge Engineering* 2001; 6: 285-293.
4. Beck JL and Au S-K. Bayesian updating of structural models and reliability using Markov chain Monte Carlo simulation. *Journal of engineering mechanics* 2002; 128: 380-391.

5. Beck JL and Yuen K-V. Model selection using response measurements: Bayesian probabilistic approach. *Journal of Engineering Mechanics* 2004; 130: 192-203.
6. Teughels A and De Roeck G. Structural damage identification of the highway bridge Z24 by FE model updating. *Journal of Sound and Vibration* 2004; 278: 589-610.
7. Jaishi B, Kim H-J, Kim MK, Ren W-X and Lee S-H. Finite element model updating of concrete-filled steel tubular arch bridge under operational condition using modal flexibility. *Mechanical Systems and Signal Processing* 2007; 21: 2406-2426.
8. Yuen K-V, Au SK and Beck JL. Two-stage structural health monitoring approach for phase I benchmark studies. *Journal of Engineering Mechanics* 2004; 130: 16-33.
9. Yuen KV, Beck JL and Au SK. Structural damage detection and assessment by adaptive Markov chain Monte Carlo simulation. *Structural Control and Health Monitoring* 2004; 11: 327-347.
10. Yuen K-V. *Bayesian methods for structural dynamics and civil engineering*. John Wiley & Sons, 2010.
11. Moaveni B, He X, Conte JP and Restrepo JI. Damage identification study of a seven-story full-scale building slice tested on the UCSD-NEES shake table. *Structural Safety* 2010; 32: 347-356.
12. Moaveni B, Stavridis A, Lombaert G, Conte JP and Shing PB. Finite-element model updating for assessment of progressive damage in a 3-story infilled RC frame. *Journal of Structural Engineering* 2012; 139: 1665-1674.
13. Bassoli E, Vincenzi L, D'Altri AM, de Miranda S, Forghieri M and Castellazzi G. Ambient vibration‐based finite element model updating of an earthquake‐damaged masonry tower. *Structural Control and Health Monitoring* 2018; 25: e2150.
14. Lam H, Peng H and Au S. Development of a practical algorithm for Bayesian model updating of a coupled slab system utilizing field test data. *Engineering Structures* 2014; 79: 182-194.
15. Lam H-F, Yang J and Au S-K. Bayesian model updating of a coupled-slab system using field test data utilizing an enhanced Markov chain Monte Carlo simulation algorithm. *Engineering Structures* 2015; 102: 144-155.
16. Behmanesh I and Moaveni B. Accounting for environmental variability, modeling errors, and parameter estimation uncertainties in structural identification. *Journal of Sound and Vibration* 2016; 374: 92-110.
17. Behmanesh I, Yousefianmoghadam S, Nozari A, Moaveni B and Stavridis A. Uncertainty quantification and propagation in dynamic models using ambient vibration measurements, application to a 10-story building. *Mechanical Systems and Signal Processing* 2018; 107: 502-514.
18. Song M, Yousefianmoghadam S, Mohammadi M-E, Moaveni B, Stavridis A and Wood RL. An application of finite element model updating for damage assessment of a two-story reinforced concrete building and comparison with lidar. *Structural Health Monitoring* 2017: 1475921717737970.
19. Song M, Behmanesh I, Moaveni B and Papadimitriou C. Modeling Error Estimation and Response Prediction of a 10-Story Building Model through a Hierarchical Bayesian Model Updating Framework. *Frontiers in Built Environment* 2019; 5: 7.
20. Song M, Moaveni B, Papadimitriou C and Stavridis A. Accounting for amplitude of excitation in model updating through a hierarchical Bayesian approach: Application to a two-story reinforced concrete building. *Mechanical Systems and Signal Processing* 2019; 123: 68-83.
21. Ebrahimian H, Ghahari SF, Asimaki D and Taciroglu E. Estimation of Dynamic Soil Parameters Using a Nonlinear Finite Element Model Updating Approach: Application to the Millikan Library. Earthquake Engineering & Structural Dynamics. Under Review.
22. Asgarieh E, Moaveni B and Stavridis A. Nonlinear finite element model updating of an infilled frame based on identified time-varying modal parameters during an earthquake. *Journal of Sound and Vibration* 2014; 333: 6057-6073.

23. Asgarieh E, Moaveni B, Barbosa AR and Chatzi E. Nonlinear model calibration of a shear wall building using time and frequency data features. *Mechanical Systems and Signal Processing* 2017; 85: 236-251.
24. Hoshiya M and Saito E. Structural identification by extended Kalman filter. *Journal of engineering mechanics* 1984; 110: 1757-1770.
25. Hoshiya M and Sutoh A. Kalman filter—finite element method in identification. *Journal of engineering mechanics* 1993; 119: 197-210.
26. Chatzi EN, Smyth AW and Masri SF. Experimental application of on-line parametric identification for nonlinear hysteretic systems with model uncertainty. *Structural Safety* 2010; 32: 326-337.
27. Azam SE and Mariani S. Dual estimation of partially observed nonlinear structural systems: A particle filter approach. *Mechanics Research Communications* 2012; 46: 54-61.
28. Hernandez EM, Bernal D and Caracoglia L. On‐line monitoring of wind‐induced stresses and fatigue damage in instrumented structures. *Structural Control and Health Monitoring* 2013; 20: 1291-1302.
29. Erazo K and Hernandez EM. Uncertainty quantification of state estimation in nonlinear structural systems with application to seismic response in buildings. *ASCE-ASME Journal of Risk and Uncertainty in Engineering Systems, Part A: Civil Engineering* 2015; 2: B5015001.
30. Liu L, Su Y, Zhu J and Lei Y. Data fusion based EKF-UI for real-time simultaneous identification of structural systems and unknown external inputs. *Measurement* 2016; 88: 456-467.
31. Erazo K and Nagarajaiah S. An offline approach for output-only Bayesian identification of stochastic nonlinear systems using unscented Kalman filtering. *Journal of Sound and Vibration* 2017; 397: 222-240.
32. Erazo K and Nagarajaiah S. Bayesian structural identification of a hysteretic negative stiffness earthquake protection system using unscented Kalman filtering. *Structural Control and Health Monitoring* 2018; 25: e2203.
33. Wu M and Smyth AW. Application of the unscented Kalman filter for real‐time nonlinear structural system identification. *Structural Control and Health Monitoring: The Official Journal of the International Association for Structural Control and Monitoring and of the European Association for the Control of Structures* 2007; 14: 971-990.
34. Chatzi EN and Smyth AW. The unscented Kalman filter and particle filter methods for nonlinear structural system identification with non‐collocated heterogeneous sensing. *Structural Control and Health Monitoring: The Official Journal of the International Association for Structural Control and Monitoring and of the European Association for the Control of Structures* 2009; 16: 99-123.
35. Xie Z and Feng J. Real-time nonlinear structural system identification via iterated unscented Kalman filter. *Mechanical systems and signal processing* 2012; 28: 309-322.
36. Ebrahimian H, Astroza R and Conte JP. Extended Kalman filter for material parameter estimation in nonlinear structural finite element models using direct differentiation method. *Earthquake Engineering & Structural Dynamics* 2015; 44: 1495-1522.
37. Ebrahimian H, Astroza R, Conte JP and Papadimitriou C. Bayesian optimal estimation for output‐only nonlinear system and damage identification of civil structures. *Structural Control and Health Monitoring* 2018; 25: e2128.
38. Azam SE, Chatzi E and Papadimitriou C. A dual Kalman filter approach for state estimation via output-only acceleration measurements. *Mechanical Systems and Signal Processing* 2015; 60: 866-886.
39. Azam SE, Chatzi E, Papadimitriou C and Smyth A. Experimental validation of the Kalman-type filters for online and real-time state and input estimation. *Journal of vibration and control* 2017; 23: 2494-2519.

40. Astroza R, Ebrahimian H and Conte JP. Material parameter identification in distributed plasticity FE models of frame-type structures using nonlinear stochastic filtering. *Journal of Engineering Mechanics* 2014; 141: 04014149.
41. Astroza R, Ebrahimian H, Li Y and Conte JP. Bayesian nonlinear structural FE model and seismic input identification for damage assessment of civil structures. *Mechanical Systems and Signal Processing* 2017; 93: 661-687.
42. Astroza R and Alessandri A. Effects of model uncertainty in nonlinear structural finite element model updating by numerical simulation of building structures. *Structural Control and Health Monitoring* 2019; 26: e2297.
43. Erazo K, Sen D, Nagarajaiah S and Sun L. Vibration-based structural health monitoring under changing environmental conditions using Kalman filtering. *Mechanical Systems and Signal Processing* 2019; 117: 1-15.
44. Erazo K, Moaveni B and Nagarajaiah S. Bayesian seismic strong-motion response and damage estimation with application to a full-scale seven story shear wall structure. *Engineering Structures* 2019; 186: 146-160.
45. Zheng B, Fu P, Li B and Yuan X. A robust adaptive unscented Kalman filter for nonlinear estimation with uncertain noise covariance. *Sensors* 2018; 18: 808.
46. Mehra R. Approaches to adaptive filtering. *IEEE Transactions on automatic control* 1972; 17: 693-698.
47. Zhang Q, Yang Y, Xiang Q, He Q, Zhou Z and Yao Y. Noise adaptive Kalman filter for joint polarization tracking and channel equalization using cascaded covariance matching. *IEEE Photonics Journal* 2018; 10: 1-11.
48. Yuen K-V and Kuok S-C. Online updating and uncertainty quantification using nonstationary output-only measurement. *Mechanical Systems and Signal Processing* 2016; 66: 62-77.
49. Astroza R, Alessandri A and Conte JP. A dual adaptive filtering approach for nonlinear finite element model updating accounting for modeling uncertainty. *Mechanical Systems and Signal Processing* 2019; 115: 782-800.
50. Almagbile A, Wang J and Ding W. Evaluating the performances of adaptive Kalman filter methods in GPS/INS integration. *Journal of Global Positioning Systems* 2010; 9: 33-40.
51. Akhlaghi S, Zhou N and Huang Z. Adaptive adjustment of noise covariance in Kalman filter for dynamic state estimation. In: *2017 IEEE Power & Energy Society General Meeting* 2017, pp.1-5. IEEE.
52. Julier SJ, Uhlmann JK and Durrant-Whyte HF. A new approach for filtering nonlinear systems. In: *Proceedings of 1995 American Control Conference-ACC'95* 1995, pp.1628-1632. IEEE.
53. Julier SJ and Uhlmann JK. New extension of the Kalman filter to nonlinear systems. In: *Signal processing, sensor fusion, and target recognition VI* 1997, pp.182-193. International Society for Optics and Photonics.
54. OpenSees 2.5.0. UC Berkeley.
55. Filippou FC, Bertero VV and Popov EP. Effects of bond deterioration on hysteretic behavior of reinforced concrete joints. 1983.
56. Center for Engineering Strong-Motion Data, https://strongmotioncenter.org/ (2019, 2019).
57. Gupta A and Krawinkler H. Behavior of ductile SMRFs at various seismic hazard levels. *Journal of Structural Engineering* 2000; 126: 98-107.